

Efficient numerical techniques for computing the Riesz fractional-order reaction-diffusion models arising in biology

Manal Alqhtani ^a, Kolade M. Owolabi ^{b,*}, Khaled M. Saad ^a, Edson Pindza ^c

^aDepartment of Mathematics, College of Sciences and Arts, Najran University, Najran, Saudi Arabia

^bDepartment of Mathematical Sciences, Federal University of Technology, PMB 704, Akure, Ondo State, Nigeria

^cDepartment of Mathematics and Applied Mathematics, University of Pretoria, Pretoria 002, South Africa

*Corresponding author. Email: kmowolabi@futa.edu.ng

Abstract

In this work, the solution of Riesz space fractional partial differential equations of parabolic type is considered. Since fractional-in-space operators have been applied to model anomalous diffusion or dispersion problems in the area of mathematical physics with success, we are motivated in this paper to model the standard Brownian motion with the fractional order operator in the sense of the Riesz derivative. We formulate two viable, efficient and reliable high-order approximation schemes for the Riesz derivative which incorporated both the left- and right-hand sides of the Riemann-Liouville derivatives. The proposed methods are analyzed for both stability and convergence. Finally, the methods are used to explore the dynamic richness of pattern formation in two important fractional reaction-diffusion equations that are still of recurring interest. Experimental results for different values of the fractional parameters are reported.

Keywords: Riesz operator; Subdiffusion and superdiffusion processes

2010 Mathematics Subject Classification

26A33

35B36

65M06

65M12

1. Introduction

The idea of fractional calculus is not a new topic, it is as old as the known integer order differentiation and integration [5], [25], [40], [54], [58]. In recent years, fractional derivative has been successfully applied to formulate many useful models in physics [37], [38], hydrology and geo-hydrology [6], [10], [29], [30], chemistry and system biology [1], [64], and finance [18], [55], [59], [62]. Specifically, fractional calculus has been used to describe different physical or natural phenomena which arise in the applicable areas of science include but not limited to diffusion processes [14], [32], pattern formation processes [2], [11], [46], [47], [53], signal processing [17], water wave movement [31], viscoelastic mechanisms [33], reaction-

diffusion model involving subdiffusion and superdiffusion processes [11], [46], [48], [53], among several others that are classified in [3], [4], [15], [23], [56].

Most scientific results in applied mathematics, physics and engineering fields have shown that these fractional order problems are more reliable, accurate and adequate than the known classical or standard order models, due to the known fact that derivatives and integrals with fractional orders give room for description of memory effects and hereditary behavior of various substances in physics, engineering and applied sciences [7], [37], [54]. This forms the basis for most vital information of the models with fractional or non-integer order when compared with integer-order cases, in which such effects are completely neglected or missing. In the area of mathematical physics, fractional-in-space derivatives are used to formulate anomalous dispersion or diffusion, where a particle diffuses or distributes at inconsistent rate with the standard Brownian motion model [9], [38], [43], [54]. Specifically, the formulation of the Riesz fractional operator involves both the left- and right- hand sides of the known Riemann–Liouville fractional derivatives [65].

Different numerical techniques have been suggested for various special fractional differential equations in a bid to seek for their analytical solutions, such methods include the spectral collocation method, Fourier transform method, integral transformation, variable separable method, Adomian decomposition method, and many others that are classified in [22], [52], [54]. However, the analytical findings of most fractional differential equations cannot be ascertained due to their nonlinear and nonlocal nature. Most of fractional differential equations do not have an analytical solutions or in some cases the exact solutions are too involving to be useful. For these reasons, most physical and real-life models in applied sciences and engineering are solved numerically. So it becomes very important to formulate a good numerical method which is capable of handling fractional differential equations.

It is widely known that the Riesz fractional operator plays an important role in characterizing anomalous diffusion, owing to successful applications to subdiffusive, superdiffusive and evolution problems [40], [54]. It is regarded as an effective tool for studying nonlocal and memory effects in physics, engineering and applied sciences. Based on research findings, the Riesz fractional definition was derived from the chaotic kinetics [57], [65]. Fractional Laplacian operators are known to arise naturally in the study of partial differential equations (PDEs) which are related to anomalous diffusion, where the fractional-order operator is known to have played an important role which is similar to that of the classical order Laplacian operator for ordinary diffusion [37], [39]. By replacing the Brownian motion of particles with Lévy flights [34], one gets a fractional reaction-diffusion equation expressed in terms of the fractional Laplacian operators [26], [27], [49] of orders $0 < \beta \leq 1$ or $1 < \beta \leq 2$, given as

$$\begin{aligned} u_t &= -D(-\Delta)^\beta u + F(u, t), \quad 0 < t \leq T, \\ u(x, y, 0) &= g(x, y), \quad (x, y) \in \mathcal{D}, \\ u(x, y, t) &= 0, \quad (x, y, t) \in \Phi \times T \end{aligned} \tag{1.1}$$

where $g : \mathcal{D} \rightarrow \mathbb{R}$ is a known function, $u = u(x, y, t)$ which represents the chemical or biological species at time t , in the x – and y – positions, is assumed to be smooth and continuous up to

certain orders, $D > 0$ is the diffusivity constant, $\Delta^\beta u = \frac{\partial^\beta u(x, t)}{\partial |x|^\beta}$ is the fractional Laplacian

operator of order β in one dimension. If $\beta \in (0, 1]$, we have subdiffusion process, but if $\beta \in (1, 2]$ one obtains the superdiffusion problem. The term $F(u, t)$ is nonlinear kinetics which accounts for all the local reactions. The Riesz fractional derivative with order β is defined by

$$\frac{\partial^\beta u(x, t)}{\partial |x|^\beta} = -\mathcal{C}_\beta \left({}^{RL}\mathcal{D}_{a,x}^\beta + {}^{RL}\mathcal{D}_{x,b}^\beta \right) u(x, t). \quad (1.2)$$

Where ${}^{RL}\mathcal{D}_{a,x}^\beta$ and ${}^{RL}\mathcal{D}_{x,b}^\beta$ stand for the left and right hand side of the Riemann-Liouville derivatives which are expressed in the form:

$$\begin{aligned} {}^{RL}\mathcal{D}_{a,x}^\beta u(x, t) &= \frac{1}{\Gamma(2-\beta)} \frac{d^2}{dx^2} \int_a^x \frac{u(\tau, t)}{(x-\tau)^{\beta-1}} d\tau, \\ {}^{RL}\mathcal{D}_{x,b}^\beta u(x, t) &= \frac{1}{\Gamma(2-\beta)} \frac{d^2}{dx^2} \int_x^b \frac{u(\tau, t)}{(\tau-x)^{\beta-1}} d\tau \end{aligned} \quad (1.3)$$

respectively, and $\mathcal{C}_\beta = \frac{\sec(\pi\beta/2)}{2}$. In a similar manner, the left- and right hand side Riemann-Liouville fractional integral operators of order $1 < \beta < 2$ defined by

$$\begin{aligned} {}^{RL}\mathcal{D}_{a,x}^{\beta-2} u(x, t) &= \frac{1}{\Gamma(2-\beta)} \int_a^x (x-\tau)^{1-\beta} u(\tau, t) d\tau, \\ {}^{RL}\mathcal{D}_{x,b}^{\beta-2} u(x, t) &= \frac{1}{\Gamma(2-\beta)} \int_x^b (\tau-x)^{1-\beta} u(\tau, t) d\tau, \end{aligned} \quad (1.4)$$

where $\Gamma(\cdot)$ denoted the Euler's Gamma function expressed as

$$\Gamma(\alpha) = \int_0^\infty \exp(-t) t^{\alpha-1} dt, \quad \alpha > 0.$$

Many authors have proposed different numerical schemes for solving the Riesz fractional differential equation of the form (1.1). For example, Zhang and Liu [67] suggested the fundamental and basic solutions of the Riesz-space fractional partial differential equations (RFPDE) in space and time, subject to the periodic conditions. In a similar development, a Galarkin based finite element approximation technique with symmetric property was developed in [68] to solve RFPDE. Different methods based on the Fourier spectral techniques was introduced and applied for numerical integration of the Riesz fractional-in-space reaction-advection-diffusion problems in one and high dimensions [16], [50], [53], and references therein.

The remaining parts of this paper are organized as follows. In Section 2 we briefly present a tour of some existing numerical methods which have been used to approximate the Riesz fractional operator. The nature of problem introduced in (1.1) permits the use of different numerical techniques in space and time, as a result, we are proposing higher-order numerical methods based of difference operators on a finite domain for the approximation of the Riesz fractional derivative in space. We also discuss convergence of this method in Section 3. Applicability of the suggested numerical technique is tested in 4 on various practical problems arising in physics and applied sciences. Conclusion is given in the last section.

2. Preliminaries

In this section, we provide some of the definitions and related results, as well as the existing numerical approximation techniques for the Riesz fractional derivative [44].

Definition 2.1

Let $u(x)$ be a smooth function defined on $(a, b) \subseteq \mathbb{R}$, the left- and right-sided Riemann-Liouville fractional order γ derivatives are defined by [25], [28], [58].

$${}^{RL}D_{a,x}^{\gamma}u(x) = \frac{1}{\Gamma(m-\gamma)} \frac{d^m}{dx^m} \int_a^x \frac{u(t)}{(x-t)^{\gamma-m+1}} dt, \quad a < x < b \quad (2.5)$$

And

$${}^{RL}D_{x,b}^{\gamma}u(x) = \frac{(-1)^m}{\Gamma(m-\gamma)} \frac{d^m}{dx^m} \int_x^b \frac{u(t)}{(t-x)^{\gamma-m+1}} dt, \quad a < x < b \quad (2.6)$$

respectively, with $m \in \mathbb{Z}^+$ satisfying $m - 1 \leq \gamma < m$.

Definition 2.2

The Fourier transform of $u(x)$ defined on \mathbb{R} is [25].

$$\widehat{u}(\tau) \cong \mathcal{F}\{u(x); \tau\} = \int_{\mathbb{R}^n} u(x) \exp(i\tau \cdot x) dx, \quad x, \tau \in \mathbb{R}^n, \quad i^2 = -1 \quad (2.7)$$

And the inverse Fourier transform is defined as

$$u(x) = \frac{1}{(2\pi)^n} \int_{\mathbb{R}^n} \widehat{u}(\tau) \exp(-i\tau \cdot x) d\tau, \quad x, \tau \in \mathbb{R}^n, \quad i^2 = -1 \quad (2.8)$$

The inner product of τ and x is denoted by $\tau \cdot x$ here.

Definition 2.3

The Fourier transform of the left- and right-sided Riemann-Liouville fractional derivatives of order γ in the interval $(a, b) = (-\infty, +\infty)$ are [28].

$$\mathcal{F}\{{}^{RL}D_{-\infty,x}^{\gamma}u(x); \tau\} = (-i\tau)^{\gamma} \widehat{u}(\tau), \quad (2.9)$$

And

$$\mathcal{F}\{ {}^{RL}D_{x,+\infty}^\gamma u(x); \tau \} = (i\tau)^\gamma \widehat{u}(\tau), \quad (2.10)$$

respectively. Here, $m-1 < \gamma < m \in \mathbb{Z}^+$, $i^2 = -1$ and $u^{(k)}(x)$ for $k = 0, 1, 2, \dots, m-1$ vanish as $x \rightarrow \pm \infty$.

According to Samko et al. [58] The Riesz derivative with a minus sign is defined as

$$\mathcal{R}_x^\beta u(x) = -\frac{{}_{-\infty}\mathcal{D}_x^\beta u(x) + {}_{+\infty}\mathcal{D}_x^\beta u(x)}{2 \cos\left(\frac{\beta\pi}{2}\right)} \quad (2.11)$$

which has the equivalence Fourier transform

$$\mathcal{F}\left\{ \mathcal{R}_x^\beta u(x) \right\} = -\frac{(i\omega)^\beta + (-i\omega)^\beta}{2 \cos\left(\frac{\beta\pi}{2}\right)} U(\omega). \quad (2.12)$$

According to [21], [40], [54].

$${}_{-\infty}\mathcal{D}_x^\beta u(x) = \frac{d^2}{dx^2} \left[{}_{-\infty}I_x^{2-\beta} u(x) \right], \quad 1 < \beta < 2$$

one writes

$$\begin{aligned} {}_{-\infty}\mathcal{D}_x^\beta u(x) &= {}_{-\infty}I_x^{2-\beta} u(x) \\ &= \frac{1}{\Gamma(2-\beta)} \frac{d^2}{dx^2} \int_{-\infty}^x \frac{u(x')}{(x-x')^{\beta-1}} dx, \\ &= \frac{1}{\Gamma(2-\beta)} \frac{d^2}{dx^2} \int_0^\infty \tau^{1-\beta} u(x-\tau) d\tau \end{aligned} \quad (2.13)$$

The γ -th order Riesz derivative for a smooth function $u(x)$ on interval $(a, b) \subseteq \mathbb{R}$ is expressed as [12], [28].

$${}^{RZ}D_x^\gamma u(x) = -\Psi_\gamma \left({}^{RL}D_{a,x}^\gamma + {}^{RL}D_{x,b}^\gamma \right) u(x) \quad (2.14)$$

where $\Psi_\gamma = \frac{1}{2 \cos(\gamma\pi/2)}$, for $\gamma \neq 1, 3, \dots$

Next, we consider the Fourier transform as one of the properties of the Riesz operator. Let a suitably smooth function $u(x) \in \mathcal{S}(\mathbb{R})$, then

$$\mathcal{F}\{ {}^{RZ}D_x^\gamma u(x); \tau \} = -|\tau|^\gamma \widehat{u}(\tau), \quad \gamma > 0. \quad (2.15)$$

By using the information in (2.14) in conjunction with formulae (2.9) and (2.10) leads to

$$\mathcal{F}\{{}^{RZ}D_x^\gamma u(x); \tau\} = -\frac{1}{2 \cos\left(\frac{\gamma\pi}{2}\right)} [(-i\tau)^\gamma \hat{u}(\tau) + (i\tau)^\gamma \hat{u}(\tau)]. \quad (2.16)$$

Bear in mind that

$$(-i)^\gamma = \exp\left(-\frac{\pi}{2}i\right)^\gamma, \quad i^\gamma = \exp\left(\frac{\pi}{2}i\right)^\gamma.$$

Therefore,

$$\mathcal{F}\{{}^{RZ}D_x^\gamma u(x); \tau\} = -\frac{|\tau|^\gamma \left(e^{-\frac{i\gamma\pi}{2}} + e^{\frac{i\gamma\pi}{2}}\right) \hat{u}(\tau)}{2 \cos\left(\frac{\gamma\pi}{2}\right)} = -|\tau|^\gamma \hat{u}(\tau), \quad (2.17)$$

where $e^{i\theta} = \cos \theta + i \sin \theta$ (Euler's formula) can be applied.

Lemma 2.4

Assume $\beta > 0$, and function $u(x, t) \in L_1(\mathbb{R})$ with respect to x , then the Fourier transform of the Riesz fractional operator is given as [54].

$$\mathcal{F}_x \left\{ \frac{\partial^\beta u(x, t)}{\partial |x|^\beta}; \rho \right\} = -|\rho|^\beta \hat{u}(\rho, t),$$

with $\hat{u}(\rho, t)$ being the Fourier transform of $u(p, t)$ w.r.t x , then

$$\hat{u}(\rho, t) = \mathcal{F}_x \{w(x, t); \rho\} = \int_{\mathbb{R}} \exp(i\rho x) u(x, t) dx, \quad \text{for } i^2 = -1.$$

Next, we follow the Ortigueira [41], [42] proposed fractional centered finite difference method for $\beta > -1$,

$$\Delta_{\hbar}^\beta u(x, t) = \sum_{k=-\infty}^{\infty} \omega_k^{(\beta)} u(x - k\hbar, t). \quad (2.18)$$

It is also proved that

$$\lim_{\hbar \rightarrow 0} \left(\frac{\Delta_{\hbar}^\beta u(x, t)}{\hbar^\beta} \right) = \lim_{\hbar \rightarrow 0} \left(-\frac{1}{\hbar^\beta} \sum_{k=-\infty}^{\infty} \omega_k^{(\beta)} u(x - k\hbar, t) \right) = \frac{\partial^\beta u(x, t)}{\partial |x|^\beta}, \text{ for } 1 < \beta < 2,$$

Where

$$\omega_k^{(\beta)} = \frac{(-1)^k \Gamma(\beta=1)}{\Gamma\left(\frac{\beta}{2} - k + 1\right) \Gamma\left(\frac{\beta}{2} + k + 1\right)}.$$

The fractional centered difference operator illustrated above is often regarded as the generalized second-order centered difference operator

$$\lim_{\beta \rightarrow 2} \Delta_{\hbar}^{\beta} u(x, t) = u(x - \hbar, t) - 2u(x, t) + u(x + \hbar, t).$$

It was reported in [41] that the associated generating coefficient $\omega_k^{(\beta)}$ arising from (2.18) are

either $\left| 2 \sin\left(\frac{\rho \hbar}{2}\right) \right|^{\beta}$ or $\left(2 - z - \frac{1}{z}\right)^{\frac{\beta}{2}}$ for $|z| < 1$, which implies,

$$\left| 2 \sin\left(\frac{\rho \hbar}{2}\right) \right|^{\beta} = \sum_{k=-\infty}^{\infty} \omega_k^{(\beta)} \exp(ik\rho \hbar),$$

or

$$\omega_0^{(\beta)} = \frac{\Gamma(\beta+1)}{\Gamma\left(\frac{\beta}{2}+1\right)} > 0, \quad \omega_k^{(\beta)} = \left(1 - \frac{\beta+1}{\frac{\beta}{2}+k}\right) \omega_{k-1}^{(\beta)} < 0, \quad k = \pm(1, 2, \dots).$$

It is obvious that $0 < 1 - \frac{\beta+1}{\frac{\beta}{2}+k}$ for $k \geq 2$, and $1 - \frac{\beta+1}{\frac{\beta}{2}+k} > 1$ for $k < -1$, so for fixed $\beta \in (1, 2)$, one obtains

$$\omega_k^{(\beta)} > \omega_{k-1}^{(\beta)} > \dots > \omega_{k-\zeta}^{(\beta)} > \dots, \quad k = 2, 3, \dots, \zeta \geq 1, k - \zeta \geq 1,$$

and

$$\omega_k^{(\beta)} < \omega_{k-1}^{(\beta)} < \dots < \omega_{k-\zeta}^{(\beta)} < \dots, \quad k = -1, -2, \dots, \zeta \leq 1, k - \zeta \leq -2.$$

In this part, a quick report some of the existing numerical approximation techniques for the Riesz derivative is presented. To start with, we define the mesh points $x_j = a + jh$, $j = 0, 1, 2, \dots, J$, and $t_k = kh$, $k = 0, 1, 2, \dots, K$, where $h = (b - a)/J$ and $\hbar = T/K$, h and \hbar denote the spatial step-size and temporal step-size, respectively.

For every β , ($1 < \beta < 2$) the left- and right- side of the Riemann-Liouville derivatives corresponds to the left- and right-hand-side of the Grwald-Letnikov (GL) fractional derivatives, respectively under certain conditions. The left and right GL operators are respectively defined as [19], [25], [54].

$$\begin{aligned}
{}^{GL}\mathcal{D}_{a,x}^\beta u(x_j, t) &= \frac{1}{h^\beta} \sum_{s=0}^m \omega_s^{(\beta)} u(x_{j-s}, t) + \mathcal{O}(h), \\
{}^{GL}\mathcal{D}_{x,b}^\beta u(x_j, t) &= \frac{1}{h^\beta} \sum_{s=0}^{J-j} \omega_s^{(\beta)} u(x_{j+s}, t) + \mathcal{O}(h),
\end{aligned} \tag{2.19}$$

where

$$\omega_s^{(\beta)} = (-1)^s \binom{\beta}{s} = \frac{(-1)^s \Gamma(1+\beta)}{\Gamma(1+s)\Gamma(1+\beta-s)}.$$

The Riesz fractional derivative has been discretized by the following methods.

Based upon the Grünwald-Letnikov standard technique, using the definition in (1.2) and the assumption above, the first order approximation to the Riesz operator is given as

$$\frac{\partial^\beta u(x_j, t)}{\partial |x|^\beta} = -\frac{\mathcal{C}_\beta}{h^\beta} \left[\sum_{s=0}^j \omega_s^{(\beta)} u(x_{j-s}, t) + \sum_{s=0}^{J-j} \omega_s^{(\beta)} u(x_{j+s}, t) \right] + \mathcal{O}(h). \tag{2.20}$$

The authors in [35] suggested a better version of the standard Grünwald-Letnikov method which was labeled as the Shifted Grünwald-Letnikov approximation scheme for the left and right (LR) Riemann-Liouville fractional derivatives in which the issue of numerical instability with the formal was circumvented, as:

$$\begin{aligned}
{}^{GL}\mathcal{D}_{a,x}^\beta u(x_j, t) &= \sum_{s=0}^{j+1} \omega_s^{(\beta)} u(x_{j-s+1}, t) + \mathcal{O}(h), \\
{}^{GL}\mathcal{D}_{x,b}^\beta u(x_j, t) &= \sum_{s=0}^{J-j+1} \omega_s^{(\beta)} u(x_{j+s-1}, t) + \mathcal{O}(h).
\end{aligned} \tag{2.21}$$

The improved first-order method of approximation is given as:

$$\frac{\partial^\beta u(x_j, t)}{\partial |x|^\beta} = -\frac{\mathcal{D}_\beta}{h^\beta} \left[\sum_{s=0}^{j+1} \omega_s^{(\beta)} u(x_{j-s+1}, t) + \sum_{s=0}^{J-j+1} \omega_s^{(\beta)} u(x_{j+s-1}, t) \right] + \mathcal{O}(h).$$

By applying the novel L_2 scheme, the left- and right- Riemann-Liouville operators of order $1 < \beta < 2$ are expressed as

$$\begin{aligned}
& {}^{RL}\mathcal{D}_{a,x}^\beta u(x,t) \\
&= \sum_{s=0}^1 \frac{x^{s-\beta}}{\Gamma(s+1-\beta)} \frac{\partial^s u(a,t)}{\partial x^s} + \frac{1}{\Gamma(2-\beta)} \int_a^x \frac{\partial^2 u(\tau,t)}{\partial \tau^2} (x-\tau)^{1-\tau} d\tau, \\
& {}^{RL}\mathcal{D}_{x,b}^\beta u(x,t) \\
&= \sum_{s=0}^1 \frac{(b-x)^{s-\beta}}{\Gamma(s+1-\beta)} \frac{\partial^s u(b,t)}{\partial x^s} + \frac{1}{\Gamma(2-\beta)} \int_a^x \frac{\partial^2 u(\tau,t)}{\partial \tau^2} (\tau-x)^{1-\tau} d\tau.
\end{aligned} \tag{2.22}$$

Therefore, the first-order method for the LR Riemann-Liouville fractional order operators [63].

$$\begin{aligned}
& {}^{RL}\mathcal{D}_{a,x}^\beta u(x_j,t) \\
&= \frac{1}{\Gamma(3-\beta)h^\beta} \left\{ \frac{(1-\beta)(2-\beta)u(x_0,t)}{j^\beta} + \frac{(2-\beta)[u(x_1,t)-u(x_0,t)]}{j^{\beta-1}} + \right. \\
& \left. \sum_{s=0}^{j-1} d_s^{(\beta)} [u(x_{j-s+1},t) - 2u(x_{j-s},t) + u(x_{j-s-1}))] \right\} \\
& \quad + \mathcal{O}(h), \\
& {}^{RL}\mathcal{D}_{x,b}^\beta u(x_j,t) \\
&= \frac{1}{\Gamma(3-\beta)h^\beta} \left\{ \frac{(1-\beta)(2-\beta)u(x_J,t)}{(J-j)^\beta} \right. \\
& \quad + \frac{(2-\beta)[u(x_J,t)-u(x_{J-1},t)]}{J-j^{\beta-1}} + \\
& \left. \sum_{s=0}^{J-j-1} d_s^{(\beta)} [u(x_{j+s-1},t) - 2u(x_{j+s},t) + u(x_{j+s+1}))] \right\} \\
& \quad + \mathcal{O}(h),
\end{aligned} \tag{2.23}$$

where $d_s^{(\beta)} = (s+1)^{2-\beta} - s^{2-\beta}$, for $s = 0, 1, 2, \dots, j-1$ or $s = 0, 1, 2, \dots, J-j-1$.

By using the definition in (1.2) and above formulas, we obtain

$$\begin{aligned}
& -\frac{\mathcal{C}_\beta}{\Gamma(3-\beta)h^\beta} \left\{ \frac{(1-\beta)(2-\beta)u(x_0,t)}{j^\beta} + \frac{(2-\beta)[u(x_1,t)-u(x_0,t)]}{j^{\beta-1}} \right. \\
& + \sum_{s=0}^{j-1} d_s^{(\beta)} [u(x_{j-s+1},t) - 2u(x_{j-s},t) + u(x_{j-s-1}))] \\
\frac{\partial^\beta u(x_j,t)}{\partial |x|^\beta} = & + \frac{(1-\beta)(2-\beta)u(x_J,t)}{(J-j)^\beta} + \frac{(2-\beta)[u(x_J,t)-u(x_{J-1},t)]}{J-j^{\beta-1}} \\
& \left. + \sum_{s=0}^{J-j-1} d_s^{(\beta)} [u(x_{j+s-1},t) - 2u(x_{j+s},t) + u(x_{j+s+1}))] \right\} + \mathcal{O}(h), \tag{2.24}
\end{aligned}$$

In [41], a fourth-order centered finite difference formula was constructed to approximate the Riesz operator as:

$$\Delta_h^\beta u(x,t) = \sum_{s=-\infty}^{\infty} \frac{(-1)^s \Gamma(\beta+1)}{\Gamma((\beta/2)-s+1)\Gamma((\beta/2)+s+1)} u(x-sh,t), \tag{2.25}$$

with equivalence relation [13].

$$\frac{\partial^\beta u(x_j,t)}{\partial |x|^\beta} = -\frac{1}{h^\beta} \Delta_h^\beta u(x_j,t) + \mathcal{O}(h^2). \tag{2.26}$$

The second-order approximations based on the shifted and weighted Grünwald-Lentikov methods for the L-R Riemann-Liouville (R-L) derivatives are [61]:

$$\begin{aligned}
& {}^{RL}\mathcal{D}_{a,x}^\beta u(x_j,t) \\
& = \frac{\mu_1}{h^\beta} \sum_{s=0}^{j+\rho_1} \omega_s^{(\beta)} u(x_{j-s+\rho_1},t) + \frac{\mu_2}{h^\beta} \sum_{s=0}^{j+\rho_2} \omega_s^{(\beta)} u(x_{j-s+\rho_2},t) + \mathcal{O}(h^2), \\
& {}^{RL}\mathcal{D}_{x,b}^\beta u(x_j,t) \\
& = \frac{\mu_1}{h^\beta} \sum_{s=0}^{J-j+\rho_1} \omega_s^{(\beta)} u(x_{j+s-\rho_1},t) + \frac{\mu_2}{h^\beta} \sum_{s=0}^{J-j+\rho_2} \omega_s^{(\beta)} u(x_{j+s-\rho_2},t) \\
& + \mathcal{O}(h^2), \tag{2.27}
\end{aligned}$$

where

$$\mu_1 = \frac{(\beta-2\rho_2)}{2(\rho_1-\rho_2)} \quad \text{and} \quad \mu_2 = \frac{(2\rho_1-\beta)}{2(\rho_1-\rho_2)}.$$

ρ_1 and ρ_2 are integers to be chosen arbitrarily.

Also, the third-order Shifted Grünwald-Lentikov schemes for the discretization of the L-R RL fractional derivatives are

$$\begin{aligned}
{}^{RL}\mathcal{D}_{a,x}^\beta u(x_j, t) &= \frac{\gamma_1}{h^\beta} \sum_{s=0}^{j+\rho_1} \omega_s^{(\beta)} u(x_{j-s+\rho_1}, t) + \frac{\gamma_2}{h^\beta} \sum_{s=0}^{j+\rho_2} \omega_s^{(\beta)} u(x_{j-s+\rho_2}, t) \\
&\quad + \frac{\gamma_3}{h^\beta} \sum_{s=0}^{j+\rho_3} \omega_s^{(\beta)} u(x_{j-s+\rho_3}, t) + \mathcal{O}(h^3), \\
{}^{RL}\mathcal{D}_{x,b}^\beta u(x_j, t) &= \frac{\gamma_1}{h^\beta} \sum_{s=0}^{J-j+\rho_1} \omega_s^{(\beta)} u(x_{j+s-\rho_1}, t) + \frac{\gamma_2}{h^\beta} \sum_{s=0}^{J-j+\rho_2} \omega_s^{(\beta)} u(x_{j+s-\rho_2}, t) \\
&\quad + \frac{\gamma_3}{h^\beta} \sum_{s=0}^{J-j+\rho_3} \omega_s^{(\beta)} u(x_{j+s-\rho_3}, t) + \mathcal{O}(h^3),
\end{aligned} \tag{2.28}$$

Where

$$\begin{aligned}
\gamma_1 &= \frac{3\beta^2 - (6\rho_3 + 6\rho_2 + 1)\beta + 12\rho_3\rho_2}{12(\rho_3\rho_2 - \rho_1\rho_2 - \rho_1\rho_3 + \rho_1^2)}, \\
\gamma_2 &= \frac{3\beta^2 - (6\rho_3 + 6\rho_1 + 1)\beta + 12\rho_1\rho_3}{12(\rho_3\rho_1 - \rho_1\rho_2 - \rho_2\rho_3 + \rho_2^2)}, \\
\gamma_3 &= \frac{3\beta^2 - (6\rho_2 + 6\rho_1 + 1)\beta + 12\rho_1\rho_2}{12(\rho_1\rho_2 - \rho_1\rho_3 - \rho_2\rho_3 + \rho_3^2)},
\end{aligned} \tag{2.29}$$

where ρ_1, ρ_2 and ρ_3 are arbitrary integers.

Finally, we presents the type I and II fractional-order centered differences definitions which was proposed by Ortigueira (2006, 2021) as follows.

Definition 2.5

Let $\beta > -1$, $h \in \mathbb{R}^+$, and $u(t)$ being a complex variable function on $(-\infty, \infty)$. The type I fractional difference is defined by [41], [42].

$$\Delta_{c_1} u(t) = \sum_{-\infty}^{+\infty} \frac{(-1)^k \Gamma(\beta+1)}{\Gamma\left(\frac{\beta}{2}-k+1\right) \Gamma\left(\frac{\beta}{2}+k+1\right)} u(t - kh) \tag{2.30}$$

With $\beta = 2M$ and $M \in \mathbb{M}^+$, the above equation transforms into

$$\Delta_{c_1}^{2M} u(t) = \sum_{-M}^{+M} \frac{(-1)^k (2M)!}{(M-k)!(M+k)!} u(t - kh). \quad (2.31)$$

called $2M$ order centered difference operator.

Definition 2.6

The type II fractional difference operator is defined by [41], [42].

$$\Delta_{c_2}^{\beta} u(t) = \sum_{-\infty}^{+\infty} \frac{(-1)^k \Gamma(\beta+1)}{\Gamma\left(\frac{\beta+1}{2} - k + 1\right) \Gamma\left(\frac{\beta-1}{2} + k + 1\right)} u\left(t - kh + \frac{h}{2}\right) \quad (2.32)$$

With $\beta = 2M + 1$, we have

$$\Delta_{c_2}^{2M+1} u(t) = \sum_{-M}^{+M} \frac{(-1)^k (2M+1)!}{(M+1-k)!(M+k)!} u\left(t - kh + \frac{h}{2}\right). \quad (2.33)$$

But if $M = 0$, we have a particular case

$$\Delta_{c_2}^1 u(t) = u\left(t + \frac{h}{2}\right) - u\left(t - \frac{h}{2}\right). \quad (2.34)$$

3. Numerical techniques for the Riesz operator

In this section, we formulate higher-order approximation schemes for the Riesz fractional diffusion equation as described in (1.1).

3.1. Fourth-order difference scheme

By adopting the Taylor's expansion, we have

$$u(x_j, t_{k-1}) = u(x_j, t_k) - \xi \frac{\partial u(x_j, t_k)}{\partial t} + \frac{\xi^2}{2} \frac{\partial^2 u(x_j, t_k)}{\partial t^2} + \mathcal{O}(\xi^3) \quad (3.35)$$

$$\frac{\partial u(x_j, t_{k-1})}{\partial t} = \frac{\partial u(x_j, t_k)}{\partial t} - \xi \frac{\partial^2 u(x_j, t_k)}{\partial t^2} + \mathcal{O}(\xi^2), \quad (3.36)$$

which when simplified results to

$$\frac{\partial^2 u(x_j, t_k)}{\partial t^2} = \frac{1}{\xi} \left(\frac{\partial u(x_j, t_k)}{\partial t} - \frac{\partial u(x_j, t_{k-1})}{\partial t} \right) + \mathcal{O}(\xi). \quad (3.37)$$

Next, we substitute for (3.37) in (3.35) to have

$$\frac{\xi}{2} \left(\frac{\partial u(x_j, t_k)}{\partial t} - \frac{\partial u(x_j, t_{k-1})}{\partial t} \right) = u(x_j, t_k) - u(x_j, t_{k-1}) + \mathcal{O}(\xi^3) \quad (3.38)$$

From above equation and (1.1), one obtains

$$\begin{aligned} 2u(x_j, t_k) - \xi D \frac{\partial^\beta u(x_j, t_k)}{\partial |x|^\beta} &= 2u(x_j, t_{k-1}) + \xi D \frac{\partial^\beta u(x_j, t_{k-1})}{\partial |x|^\beta} \\ &\quad + \xi F[(x_j, t_k) + (x_j, t_{k-1})] + \mathcal{O}(\xi^3). \end{aligned} \quad (3.39)$$

Take u^k to be approximation solution of $u(x_j, t_k)$. We substitute

$$\begin{aligned} \frac{\partial^\beta u(x_j, t_k)}{\partial |x|^\beta} &= \frac{\beta}{24h^\beta} \sum_{s=-J+j+1}^{j-1} \mu_s^{(\beta)} u(x_{j-(s+1)}, t) \\ &\quad + \frac{\beta}{24h^\beta} \sum_{s=-J+j+1}^{j-1} \mu_s^{(\beta)} u(x_{j-(s-1)}, t) \\ &\quad - \left(1 + \frac{\beta}{12}\right) \frac{1}{h^\beta} \sum_{s=-J+j+1}^{j-1} \mu_s^{(\beta)} u(x_{j-s}, t) + \mathcal{O}(h^4) \end{aligned} \quad (3.40)$$

Into (3.39) and neglecting the higher other terms to obtain the difference method

$$\begin{aligned} u_j^k - \frac{\beta \xi D}{48h^\beta} \left(\sum_{s=-J+j+1}^{j-1} \mu_s^{(\beta)} u_{j-s-1}^k + \sum_{s=-J+j+1}^{j-1} \mu_s^{(\beta)} u_{j-s+1}^k \right) \\ + \left(\frac{\xi D}{2h^\beta} \right) \left(1 + \frac{\beta}{12} \right) \sum_{s=-J+j+1}^{j-1} \mu_s^{(\beta)} u_{j-s}^k \\ = u_j^{k-1} + \frac{\beta \xi D}{48h^\beta} \left(\sum_{s=-J+j+1}^{j-1} \mu_s^{(\beta)} u_{j-s-1}^{k-1} + \sum_{s=-J+j+1}^{j-1} \mu_s^{(\beta)} u_{j-s+1}^{k-1} \right) \\ - \left(\frac{\xi D}{2h^\beta} \right) \left(1 + \frac{\beta}{12} \right) \sum_{s=-J+j+1}^{j-1} \mu_s^{(\beta)} u_{j-s}^{k-1} + \frac{\xi}{2} \left(F_j^k + F_j^{k-1} \right), \end{aligned} \quad (3.41)$$

with

$$u^k = \begin{pmatrix} u_1^k \\ u_2^k \\ \vdots \\ u_{J-1}^k \end{pmatrix} \quad \text{and} \quad F^k = \begin{pmatrix} F_1^k \\ F_2^k \\ \vdots \\ F_{J-1}^k \end{pmatrix}$$

The above difference scheme transforms into matrix form

$$\left(I + \left(\frac{\xi D}{2h^\beta} \right) A - \frac{\beta \xi D}{48h^\beta} (B + C) \right) u^k = \left(I - \left(\frac{\xi D}{2h^\beta} \right) A + \frac{\beta \xi D}{48h^\beta} (B + C) \right) u^{k-1} + \frac{\xi}{2} (F_j^k + F_j^{k-1}), \quad (3.42)$$

where I denotes the identity matrix of size $(J-1) \times (J-1)$,

$$A = \begin{bmatrix} \mu_0^{(\beta)} & \mu_{-1}^{(\beta)} & \cdots & \mu_{3-J}^{(\beta)} & \mu_{2-J}^{(\beta)} \\ \mu_1^{(\beta)} & \mu_0^{(\beta)} & \mu_{-1}^{(\beta)} & \cdots & \mu_{3-J}^{(\beta)} \\ \vdots & \ddots & \ddots & \ddots & \vdots \\ \mu_{J-3}^{(\beta)} & \cdots & \mu_1^{(\beta)} & \mu_0^{(\beta)} & \mu_{-1}^{(\beta)} \\ \mu_{J-3}^{(\beta)} & \mu_{J-4}^{(\beta)} & \cdots & \mu_1^{(\beta)} & \mu_0^{(\beta)} \end{bmatrix}, \quad B = \begin{bmatrix} 0 & \mu_0^{(\beta)} & \cdots & \mu_{4-J}^{(\beta)} & \mu_{3-J}^{(\beta)} \\ 0 & \mu_1^{(\beta)} & \mu_0^{(\beta)} & \cdots & \mu_{4-J}^{(\beta)} \\ \vdots & \ddots & \ddots & \ddots & \vdots \\ 0 & \cdots & \mu_2^{(\beta)} & \mu_1^{(\beta)} & \mu_0^{(\beta)} \\ 0 & \mu_{J-2}^{(\beta)} & \cdots & \mu_2^{(\beta)} & \mu_1^{(\beta)} \end{bmatrix},$$

$$C = \begin{bmatrix} \mu_{-1}^{(\beta)} & \mu_{-2}^{(\beta)} & \cdots & \mu_{2-J}^{(\beta)} & 0 \\ \mu_0^{(\beta)} & \mu_{-1}^{(\beta)} & \mu_{-2}^{(\beta)} & \cdots & 0 \\ \vdots & \ddots & \ddots & \ddots & \vdots \\ \mu_{J-4}^{(\beta)} & \cdots & \mu_0^{(\beta)} & \mu_{-1}^{(\beta)} & 0 \\ \mu_{J-3}^{(\beta)} & \mu_{J-4}^{(\beta)} & \cdots & \mu_0^{(\beta)} & 0 \end{bmatrix},$$

and

$$\mu_s^{(\beta)} = \frac{(-1)^s \Gamma(\beta+1)}{\Gamma[(\beta/2)-s+1] \Gamma[(\beta/2)+s+1]}, \quad s = 2 - J, 3 - J, \dots, J - 3, J - 2.$$

In what follows, we check the stability and convergence of the suggested scheme (3.42).

Theorem 3.1

The numerical scheme (3.42) is unconditionally stable.

Proof. From (3.42), we let $\mathcal{A} = \frac{\xi D}{2h^\beta} A - \frac{\beta \xi D}{48h^\beta} (B + C)$, and denote its numerical and exact solutions by u^n and u^n , respectively. Note that the matrix $(I + \mathcal{A})^{-1}$ is invertible, which means its error equation can be obtained in the form

$$\mathcal{E}^n = \mathcal{B} \mathcal{E}^{n-1}, \quad (3.43)$$

where $\mathcal{E}^n = u^n - u^n$, and $\mathcal{B} = (I + \mathcal{A})^{-1} (I - \mathcal{A})$. From above equation, we get

$$\mathcal{E}^n = \mathcal{B}^{n-1} \mathcal{E}^0. \quad (3.44)$$

Next, we give the following lemma.

Lemma 3.2

(see [66]). Let \mathcal{A} be a definite positive matrix of order $J - 1$. Then for any $\epsilon \geq 0$, the following inequalities are satisfied.

$$\|(I + \epsilon \mathcal{A})^{-1}\|_\infty \leq 1,$$

and

$$\|(I + \epsilon \mathcal{A})^{-1} (I - \epsilon \mathcal{A})\|_\infty \leq 1.$$

By applying Lemma 3.2 and (3.44), one obtains

$$\|\mathcal{E}^n\|_\infty \leq \|\mathcal{B}^{n-1}\|_\infty \|\mathcal{E}^0\|_\infty \leq$$

which implies that

$$\|\mathcal{B}\|_\infty^{n-1} \|\mathcal{E}^0\|_\infty \leq \|\mathcal{E}^0\|_\infty,$$

which shows that schemes (3.42) and its equivalence (3.41) are unconditionally stable.

Theorem 3.3

The local truncation error (LTE) analysis of method (3.41) for numerical approximation of the Riesz reaction-diffusion model (1.1) at (x_j, t_k) is given as $\mathcal{O}(\xi^2 + h^4)$, and the difference scheme is convergence of order if there exists $C > 0$ such that

$$|u(x_j, t_s) - u_j^s| \leq C(\xi^2 + h^4).$$

Proof. To begin with, we define the LTE at point (x_j, t_k) as

$$\begin{aligned}
& \frac{2}{\xi} [u(x_j, t_k) - u(x_j, t_{k-1})] + \frac{2}{\xi} \left\{ \left(\frac{\xi D}{2h^\beta} \right) \left(1 + \frac{\beta}{12} \right) \sum_{s=-J+j+1}^{j-1} \mu_s^{(\beta)} u(x_{j-s}, t_k) \right. \\
& \quad \left. - \frac{\beta \xi D}{48h^\beta} \left[\sum_{s=-J+j+1}^{j-1} \mu_s^{(\beta)} u(x_{j-s-1}, t_k) + \sum_{s=-J+j+1}^{j-1} \mu_s^{(\beta)} u(x_{j-s+1}, t_k) \right] \right\} \\
\mathcal{I}_j^k = & + \frac{2}{\xi} \left\{ \left(\frac{\xi D}{2h^\beta} \right) \left(1 + \frac{\beta}{12} \right) \sum_{s=-J+j+1}^{j-1} \mu_s^{(\beta)} u(x_{j-s}, t_{k-1}) \right. \\
& \quad - \frac{\beta \xi D}{48h^\beta} \left[\sum_{s=-J+j+1}^{j-1} \mu_s^{(\beta)} u(x_{j-s-1}, t_{k-1}) \right. \\
& \quad \left. \left. + \sum_{s=-J+j+1}^{j-1} \mu_s^{(\beta)} u(x_{j-s+1}, t_{k-1}) \right] \right\} - F(x_j, t_k) - F(x_j, t_{k-1}). \tag{3.45}
\end{aligned}$$

By applying the Taylor's expansion, one gets

$$\frac{2}{\xi} [u(x_j, t_k) - u(x_j, t_{k-1})] = \frac{\partial u(x_j, t_k)}{\partial t} + \frac{\partial u(x_j, t_{k-1})}{\partial t} + \mathcal{O}(\xi^2). \tag{3.46}$$

From eqs. (3.40), (3.46), we have

$$\begin{aligned}
\mathcal{I}_j^k & = \left(\frac{\partial u(x_j, t_k)}{\partial t} - D \frac{\partial^\beta u(x_j, t_k)}{\partial |x|^\beta} - F(x_j, t_k) \right) \\
& \quad + \left(\frac{\partial u(x_j, t_{k-1})}{\partial t} - D \frac{\partial^\beta u(x_j, t_{k-1})}{\partial |x|^\beta} - F(x_j, t_{k-1}) \right) + \mathcal{O}(\xi^2 + h^4). \tag{3.47}
\end{aligned}$$

Finally, we substitute (1.1) into (3.47) to obtain the LTE

$$\mathcal{I}_j^k = \mathcal{O}(\xi^2 + h^4).$$

In the case of convergence, we let $\delta_j^k = u(x_j, t_s)$. It directly follow from (3.41) and (3.45) that

$$\begin{aligned}
& \delta_j^k - \frac{\beta \xi D}{48h^\beta} \left(\sum_{s=-J+j+1}^{j-1} \mu_s \delta_{j-s-1}^k + \sum_{s=-J+j+1}^{j-1} \mu_s \delta_{j-s+1}^k \right) + \left(\frac{\xi D}{2h^\beta} \right) \left(1 + \frac{\beta}{12} \right) \\
& \sum_{s=-J+j+1}^{j-1} \mu_s \delta_{j-s}^k \\
& = \delta_j^{k-1} + \frac{\beta \xi D}{48h^\beta} \left(\sum_{s=-J+j+1}^{j-1} \mu_s \delta_{j-s-1}^{k-1} + \sum_{s=-J+j+1}^{j-1} \mu_s \delta_{j-s+1}^{k-1} \right) \\
& + \left(\frac{\xi D}{2h^\beta} \right) \left(1 + \frac{\beta}{12} \right) \sum_{s=-J+j+1}^{j-1} \mu_s \delta_{j-s}^{k-1} + \frac{\xi}{2} \mathcal{T}_j^k.
\end{aligned} \tag{3.48}$$

Let $d^k = (\delta_1^k, \delta_2^k, \dots, \delta_{J-1}^k)^T$ and , so that (3.48) can have matrix representation of the form

$$(I + \mathcal{A})d^k = (I - \mathcal{A})d^{k-1} + \frac{\xi}{2} \mathcal{T}^k. \tag{3.49}$$

In addition, we can have

$$\begin{aligned}
& d^k \\
& = \mathcal{B}d^{k-1} + (\xi/2)(I + \mathcal{A})^{-1} \mathcal{T}^k \\
& = \mathcal{B} \left(\mathcal{B}^{k-2} + (\xi/2)(I + \mathcal{A})^{-1} \mathcal{T}^k \right) + (\xi/2)(I + \mathcal{A})^{-1} \mathcal{T}^k \\
& \quad \vdots \\
& = (\mathcal{B}^{k-1} + \mathcal{B}^{k-2} + \dots + I)(\xi/2)(I + \mathcal{A})^{-1} \mathcal{T}^k.
\end{aligned} \tag{3.50}$$

By using the results of Theorem 3.3 and Lemma 3.2, we have

$$\begin{aligned}
\left\| (\xi/2)(I + \mathcal{A})^{-1} \mathcal{T}^k \right\|_\infty &= \left\| \frac{\xi}{2}(I + \mathcal{A})^{-1} \mathcal{T}^k \right\|_\infty \leq \frac{\xi}{2} \left\| (I + \mathcal{A})^{-1} \right\|_\infty \left\| \mathcal{T}^k \right\|_\alpha \\
&\leq \xi E(\xi^2 + h^4).
\end{aligned} \tag{3.51}$$

The combination of (3.50) and (3.51) leads to

$$\begin{aligned}
\|d^k\|_\infty &= \|(\mathcal{B}^{k-1} + \mathcal{B}^{k-2} + \dots + I)(\xi/2)(I + \mathcal{A})^{-1} \mathcal{J}^k\|_\infty \\
&\leq \|(\mathcal{B}^{k-1} + \mathcal{B}^{k-2} + \dots + I)\|_\infty \|(\xi/2)(I + \mathcal{A})^{-1} \mathcal{J}^k\|_\infty \\
&\leq \left(\|\mathcal{B}^{k-1}\|_\infty + \|\mathcal{B}^{k-2}\|_\infty + \dots + \|I\|_\infty \right) \|(\xi/2)(I + \mathcal{A})^{-1} \mathcal{J}^k\|_\infty \\
&\leq \left(\|\mathcal{B}\|_\infty^{k-1} + \|\mathcal{B}\|_\infty^{k-2} + \dots + \|I\|_\infty \right) \|\mathcal{W}\|_\infty \\
&\leq k\xi E(\xi^2 + h^4),
\end{aligned} \tag{3.52}$$

where $\mathcal{W} = (\xi/2)(I + \mathcal{A})^{-1} \mathcal{J}^k$. Bear in mind that $k\xi \leq K\xi = T$, we have.

$$\|d^k\|_\infty \leq TE(\xi^2 + h^4)$$

Theorem 3.4

Assume $u \in C^7(\mathbb{R})$ with all derivatives up-to the seventh-order are in $L_1(\mathbb{R})$. Then

$$\frac{\partial^\beta u(x)}{\partial |x|^\beta} = -\hbar^{-\beta} \sum_{\tau=-1}^1 \mathcal{A}_\tau^{(\beta)} \mathcal{B}_\tau^{(\beta)} u(x) + \mathcal{O}(\hbar^4), \tag{3.53}$$

as $\hbar \rightarrow 0$ and $\frac{\partial^\beta u(x)}{\partial |x|^\beta}$ is the Riesz fractional operator for which $\beta \in (0, 1)$ and $\beta \in (1, 2]$ which correspond to sub-diffusive and super-diffusive processes, respectively.

Proof. Assume

$$\delta(x, \hbar) = \frac{\partial^\beta u(x)}{\partial |x|^\beta} + \hbar^{-\beta} \sum_{\tau=-1}^1 \mathcal{A}_\tau^{(\beta)} \mathcal{B}_\tau^{(\beta)} u(x) \tag{3.54}$$

By applying the Fourier transformation expressed as [53].

$$\hat{u}(\xi) = \mathcal{F}\{u(x)\} = \int_{-\infty}^{\infty} e^{-i\xi x} u(x) dx, \quad \text{for } \xi \in \mathbb{R},$$

then (3.54) becomes

$$\begin{aligned}
&\hat{\delta}(\xi, \hbar) \\
&= -|\xi|^\beta \hat{u}(\xi) - \left[\frac{\beta}{24} \sum_{k=-\infty}^{\infty} \frac{\eta_k^{(\beta)} e^{-i(k-1)\xi\hbar}}{\hbar^\beta} - \left(\frac{\beta}{12} + 1 \right) \sum_{k=-\infty}^{\infty} \frac{\eta_k^{(\beta)} e^{-ik\xi\hbar}}{\hbar^\beta} + \frac{\beta}{24} \sum_{k=-\infty}^{\infty} \frac{\eta_k^{(\beta)} e^{-i(k+1)\xi\hbar}}{\hbar^\beta} \right]
\end{aligned} \tag{3.55}$$

Bear in mind that the coefficients $\eta_k^{(\beta)}$ for $k \in \mathbb{Z}$ satisfy $\left|2 \sin \frac{z}{2}\right|^\beta = \sum_{-\infty}^{\infty} \eta_k^{(\beta)} e^{-ikz}$, so that the relation above can be written as

$$\hat{\delta}(\xi, \hbar) = \left[-|\xi|^\beta - \left(\frac{\beta}{12} \cos \xi \hbar - \left(\frac{\beta}{12} \right) \right) \left| \frac{2 \sin\left(\frac{\xi \hbar}{2}\right)}{\hbar} \right|^\beta \right] \hat{u}(\xi) \quad (3.56)$$

Again, based on Taylor's expansion, one obtains the relation of the function $\sin(\xi \hbar/2)$ at center $\xi = 0$ as

$$\left| \frac{2 \sin\left(\frac{\xi \hbar}{2}\right)}{\hbar} \right|^\beta = \left[|\xi|^\beta \left[1 - \frac{\beta}{24} (\xi \hbar)^2 \left(\frac{1}{1920} + \frac{\beta-1}{1152} \right) \beta (\xi \hbar)^4 - \left(\frac{1}{322560} + \frac{\beta-1}{46080} + \frac{(\beta-1)(\beta-2)}{82944} \right) \beta (\xi \hbar)^6 + \mathcal{O}\left((\xi \hbar)^8\right) \right] \right] \quad (3.57)$$

By substituting for (3.57) in (3.56), one obtains

$$\hat{\delta}(\xi, \hbar) = |\xi|^\beta \left[\frac{\beta}{288} - \frac{\beta^2}{576} + \frac{\beta}{1920} + \frac{\beta(\beta-1)}{1152} \right] (\xi \hbar)^4 \hat{u}(\xi) + \mathcal{O}\left((\xi \hbar)^6\right). \quad (3.58)$$

It should be recalled that since $u \in C^7(\mathbb{R})$, there exists $C_0 > 0$ (a constant) such that

$$|\hat{u}(\xi)| \leq C_0 (1 + |\xi|)^{-7}. \quad (3.59)$$

Hence, from eqs. (3.58), (3.59), we have

$$\begin{aligned} |\hat{\delta}| &\leq C \hbar^4 |\xi|^{4+\beta} C_0 (1 + |\xi|)^{-7} \\ &\leq C \hbar^4 (1 + |\xi|)^{4+\beta} (1 + |\xi|)^{-7} \\ &= C \hbar^4 (1 + |\xi|)^{\beta-3}, \end{aligned} \quad (3.60)$$

where $C = CC_0$ does not depend on ζ . This implies that the inverse Fourier transform of the function $\hat{\delta}(\xi, \hbar)$ holds for all $\beta \in (0, 1)$ and $\beta \in (1, 2]$. By using (3.60) and taking the inverse Fourier transform of (3.55) leads to

$$\begin{aligned}
|\delta(x, \hbar)| &\leq \frac{1}{2\pi} \int_{-\infty}^{\infty} |\hat{\delta}(\xi, \hbar)| d\xi \\
&\leq \int_{-\infty}^{\infty} C\hbar^4 (1+|\xi|)^{\beta-3} d\xi \\
&= \frac{C}{(2-\beta)\pi} \hbar^4.
\end{aligned} \tag{3.61}$$

Therefore, $\delta(x, \hbar) = \mathcal{O}(\hbar^4)$.

3.2. Improved fourth-order alternating direction implicit method of Crank-Nicolson type

In this segment, we modify a high-order centered difference method for two-dimensional Riesz space fractional reaction-diffusion equation. To achieve this, we define \mathcal{D} to be a finite domain which satisfy $\mathcal{D} = [x_L, x_R] \times [y_L, y_R]$ and $0 \leq t \leq T$. next, we utilize a uniform grid points (x_i, y_j, t_s) , $\Delta x = \frac{x_R - x_L}{P}$ and $\Delta y = \frac{y_R - y_L}{Q}$ are the spatial grid sizes in x - and y - directions, respectively, with partitions $x_i = x_L + i\Delta x$, $y_j = y_L + j\Delta y$ for $i = 0, 1, 2, \dots, P$, $j = 0, 1, 2, \dots, Q$, and $\Delta t = T/N$ is the time-step with partition $t_n = n\Delta t$ for $n = 0, 1, 2, \dots, N$, where P , Q and N are all positive integers.

By applying the modified fractional centered difference operator to discretize the Riesz derivatives, and based on Theorem 3.4, we obtained the following discretization schemes

$$\frac{\partial^\beta u(x_i, y_j, t)}{\partial |x|^\beta} = -\Delta x^{-\beta} \sum_{\tau=-1}^1 \mathcal{A}_\tau^{(\beta)} \sum_{k=-\infty}^{\infty} \eta_k^{(\beta)} u(x_{i-k-\tau}, y_j, t) + \mathcal{O}(\Delta x^4), \quad \beta \in (1, 2], \tag{3.62}$$

similarly,

$$\frac{\partial^\beta u(x, y_j, t)}{\partial |y|^\beta} = -\Delta y^{-\beta} \sum_{\tau=-1}^1 \mathcal{A}_\tau^{(\beta)} \sum_{k=-\infty}^{\infty} \eta_k^{(\beta)} u(x, y_{j-k-\tau}, t) + \mathcal{O}(\Delta y^4), \quad \beta \in (1, 2]. \tag{3.63}$$

Next, we assume $u_{i,j}(t) = u(x_i, y_j, t)$ for $i = 1, 2, \dots, P-1$ and $j = 1, 2, \dots, Q-1$ subject to the zero-flux boundary conditions, the two-dimensional Riesz space fractional reaction-diffusion eq. (1.1) is resolved in time to a system of ODEs by applying the eqs. (3.62), (3.63) to have

$$\begin{aligned}
\frac{\partial u_{i,j}(t)}{\partial t} &= -D\Delta x^{-\beta} \sum_{\tau=-1}^1 \mathcal{A}_\tau^{(\beta)} \sum_{k=-P+i}^i \eta_k^{(\beta)} u_{i-k-\tau,j}(t) \\
&\quad -D\Delta y^{-\beta} \sum_{\tau=-1}^1 \mathcal{A}_\tau^{(\beta)} \sum_{k=-Q+j}^j \eta_k^{(\beta)} u_{i,j-k-\tau}(t) + F(u_{i,j}(t)),
\end{aligned} \tag{3.64}$$

and for the sake of simplicity, we let $\theta = i - k - \tau$ and $\vartheta = j - k - \tau$, so that

$$\begin{aligned}
\frac{\partial u_{i,j}(t)}{\partial t} &= -D \sum_{\tau=-1}^1 \mathcal{A}_\tau^{(\beta)} \left(\sum_{\theta=-\tau+P}^{-\tau} \frac{\eta_{i-\theta-\tau}^{(\beta)}}{\Delta x^\beta} u_{\theta,j}(t) + \sum_{\theta=-\tau+Q}^{-\tau} \frac{\eta_{i-\theta-\tau}^{(\beta)}}{\Delta y^\beta} u_{i,\vartheta}(t) \right) \\
&\quad + F(u_{i,j}(t))
\end{aligned} \tag{3.65}$$

For computational convenience, the two operators above can be denoted as

$$\mathcal{D}_{\beta,x} u_{i,j}^n = \sum_{\tau=-1}^1 \mathcal{A}_\tau^{(\beta)} \sum_{\theta=-\tau+P}^{-\tau} \frac{\eta_{i-\theta-\tau}^{(\beta)}}{\Delta x^\beta} u_{\theta,j}^n, \quad \text{and} \quad \mathcal{D}_{\beta,y} u_{i,j}^n = \sum_{\tau=-1}^1 \mathcal{A}_\tau^{(\beta)} \sum_{\theta=-\tau+Q}^{-\tau} \frac{\eta_{i-\theta-\tau}^{(\beta)}}{\Delta y^\beta} u_{i,\vartheta}^n$$

A Crank-Nicolson version of finite difference equation for the 2D Riesz space fractional reaction-diffusion eq. (1.1) can be formulated by substituting the improved version of fractional centered difference approximations into the given differential equation at time as $t_{n+\frac{1}{2}} = \frac{1}{2}(t_{n+1} + t_n)$ as [60].

$$\frac{u_{i,j}^{n+1} - u_{i,j}^n}{\Delta t} = -D(\mathcal{D}_{\beta,x} + \mathcal{D}_{\beta,y}) \frac{u_{i,j}^{n+1} + u_{i,j}^n}{2} + \frac{f_{i,j}^{n+1} + f_{i,j}^n}{2} \tag{3.66}$$

At this stage, we can rearrange eq. (3.66) and rewrite it in the form

$$\left[\mathcal{I} + \frac{\Delta t}{2} D(\mathcal{D}_{\beta,x} + \mathcal{D}_{\beta,y}) \right] u_{i,j}^{n+1} = \left[\mathcal{I} - \frac{\Delta t}{2} D(\mathcal{D}_{\beta,x} + \mathcal{D}_{\beta,y}) \right] u_{i,j}^n + f_{i,j}^{n+\frac{1}{2}} \Delta t, \tag{3.67}$$

where \mathcal{I} denotes the identity operator, and $f_{i,j}^{n+\frac{1}{2}} = \frac{f_{i,j}^{n+1} + f_{i,j}^n}{2}$. By ignoring the higher-order terms, the fractional difference scheme (3.67) becomes

$$\begin{aligned}
&\left[\mathcal{I} + \frac{\Delta t}{2} D(\mathcal{D}_{\beta,x}) \right] \left[\mathcal{I} + \frac{\Delta t}{2} D(\mathcal{D}_{\beta,y}) \right] u_{i,j}^{n+1} \\
&= \left[\mathcal{I} - \frac{\Delta t}{2} D(\mathcal{D}_{\beta,x}) \right] \left[\mathcal{I} - \frac{\Delta t}{2} D(\mathcal{D}_{\beta,y}) \right] u_{i,j}^n + f_{i,j}^{n+\frac{1}{2}} \Delta t
\end{aligned} \tag{3.68}$$

In order to implement the scheme, we follow the strategy adopted in [52] by denoting a solution computed at intermediate time as u^* , to obtain

$$\begin{aligned} \left[\mathcal{J} + \frac{\Delta t}{2} D(\mathcal{D}_{\beta,x}) \right] u_{i,j}^* &= \left[\mathcal{J} - \frac{\Delta t}{2} D(\mathcal{D}_{\beta,y}) \right] u_{i,j}^n + f_{i,j}^{n+\frac{1}{2}} \Delta t \\ \left[\mathcal{J} + \frac{\Delta t}{2} D(\mathcal{D}_{\beta,y}) \right] u_{i,j}^{n+1} &= \left[\mathcal{J} - \frac{\Delta t}{2} D(\mathcal{D}_{\beta,x}) \right] u_{i,j}^* + f_{i,j}^{n+\frac{1}{2}} \Delta t \end{aligned} \quad (3.69)$$

Theorem 3.5

The alternating direction implicit Crank-Nicolson (ADICN) scheme (3.68) formulated to discretize the Riesz fractional eq. (1.1) is consistent with a truncation error of order $\mathcal{O}(\Delta x^4) + \mathcal{O}(\Delta y^4) + \mathcal{O}(\Delta t^2)$.

Proof. It should be noted that we utilized the second order centered finite difference scheme for the temporal direction. We employ the result in Theorem 3.4 to write the accuracy in spatial directions as

$$\frac{\partial^\beta u(x_i, y_j, t_n)}{\partial |x|^\beta} = -\mathcal{D}_{\beta,x} u_{i,j}^n + \mathcal{O}(\Delta x^4), \quad \frac{\partial^\beta u(x_i, y_j, t_n)}{\partial |y|^\beta} = -\mathcal{D}_{\beta,y} u_{i,j}^n + \mathcal{O}(\Delta x^4) \quad (3.70)$$

So the ADICN scheme is second-order accurate in time and fourth-order accurate in space.

Theorem 3.6

The ADICN method defined by (3.68) for solving the 2D Riesz fractional eq. (1.1) is unconditionally stable.

Before going to the application section, there is need to test the accuracy and applicability of the proposed scheme. As a result, we consider the following Riesz fractional diffusion equation

$$\frac{\partial u(x,t)}{\partial t} = D_u \frac{\partial^\beta u(x,t)}{\partial |x|^\beta} + F(x,t), \quad 0 < x < 1, \quad 0 < t \leq 1, \quad (3.71)$$

where

$$\begin{aligned} &(2\beta + 1)t^{2\beta} x^4 (1-x)^4 + t^{2\alpha+1} \sec(\pi\beta/2) \left(\frac{12}{\Gamma(5-\beta)} [x^{4-\beta} + (1-x)^{4-\beta}] \right. \\ F(x,t) = &-\frac{240}{\Gamma(6-\beta)} [x^{5-\beta} + (1-x)^{5-\beta}] + \frac{2160}{\Gamma(7-\beta)} [x^{6-\beta} + (1-x)^{6-\beta}] \\ &\left. - \frac{10080}{\Gamma(8-\beta)} [x^{7-\beta} + (1-x)^{7-\beta}] + \frac{20160}{\Gamma(9-\beta)} [x^{8-\beta} + (1-x)^{8-\beta}] \right), \end{aligned} \quad (3.72)$$

subject to the initial condition $u(x,0) = 0$ and zero-flux boundary conditions. It is not difficult to see that the analytic solution of the Riesz fractional eq. (3.71) is $u(x,t) = t^{2\beta+1} x^4 (1-x)^4$.

We give numerical results in the L^∞ -norm error

$$L^\infty = \max_{1 \leq j \leq N} \frac{|u_j - \bar{u}_j|}{u_j},$$

where u_j and \bar{u}_j are numerical and exact solutions, respectively. Numerical results are given with $x \in [0, 1]$, $D_u = 0.50$ and simulation time $t = 1.00$ for some values of $\beta \in (1, 2]$. The comparison between the exact and numerical solutions, as well as convergence in space is given in Fig. 1. The surface plots with different values of β is presented in Fig. 2. In Table 1, we further demonstrate the accuracy and effectiveness of the numerical method by reporting the relative error for different instances of simulation time and fractional power index β , as indicated in the table caption.

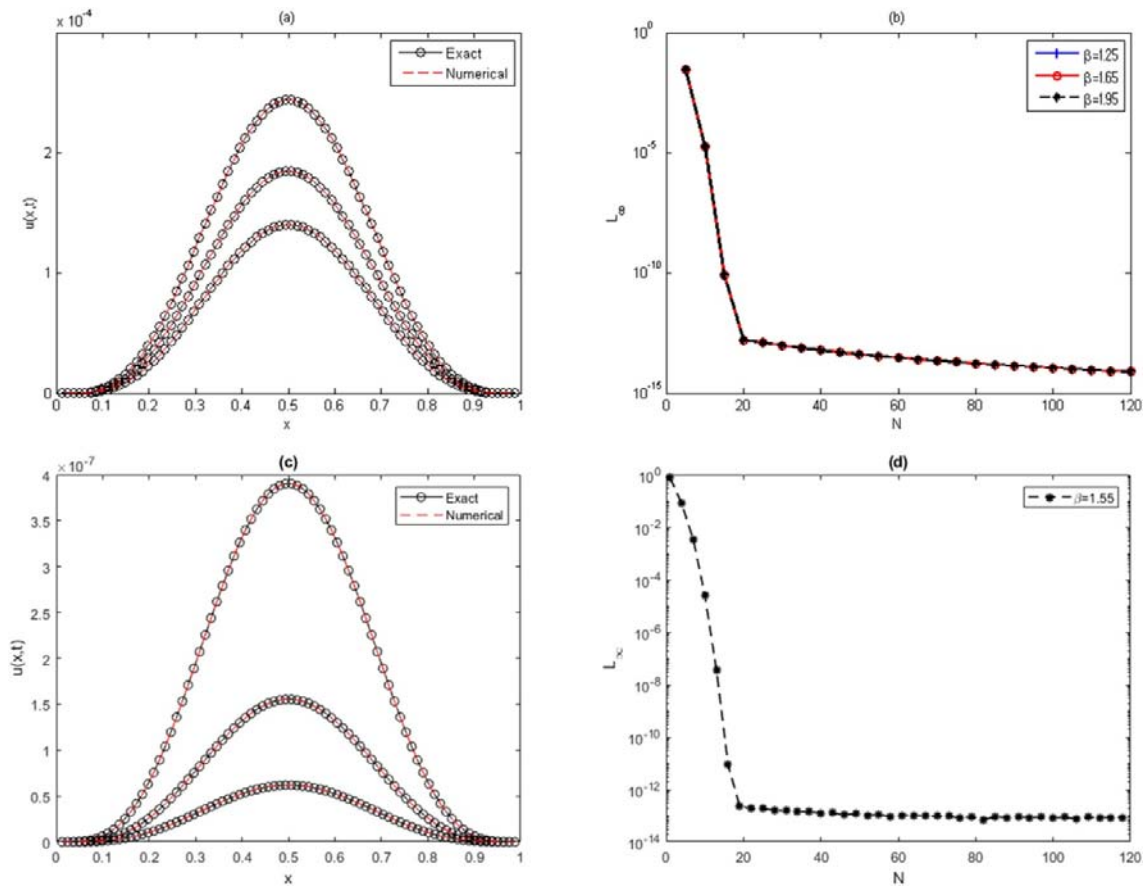


Fig. 1. Numerical results showing; (a,c) the accuracy of the proposed scheme, the upper-, middle-, and lower-plots correspond to $\beta = 1.50, 1.70, 1.90$, respectively. (b,d) convergence in space for different values of β . Upper and lower rows corresponds to numerical schemes (3.42) and (3.68), respectively.

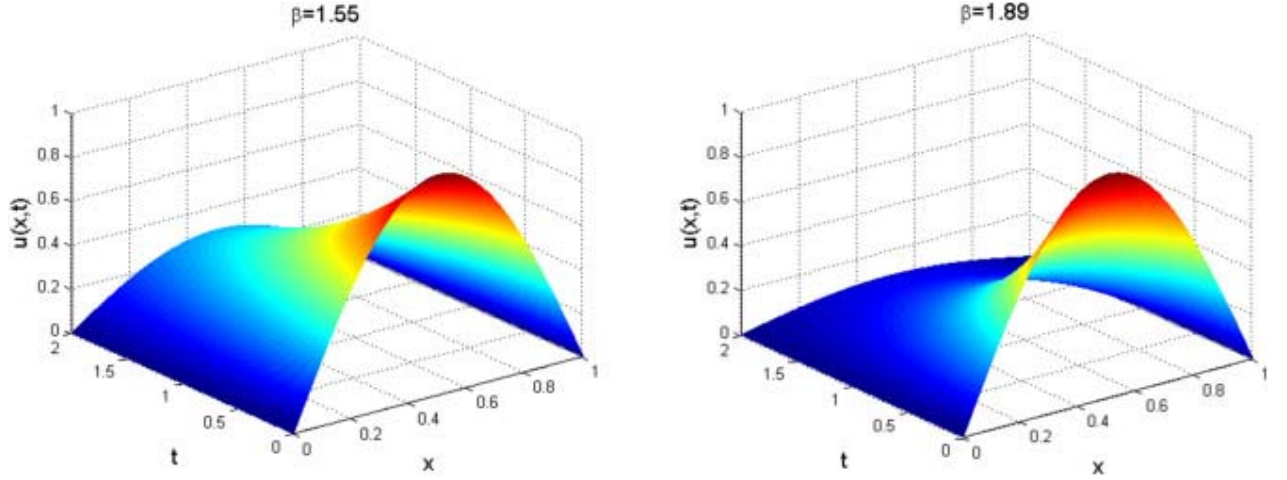


Fig. 2. Surface plots for numerical solution of (3.71) for different β as showing in the captions.

Table 1. Numerical solution of the Riesz space fractional eq. (3.71) showing the relative error and computational time results for different instances of β and final time t with $D_u = 0.850$ and $N = 80$.

β	1.10	1.30	1.50	1.70	1.90
$t = 1.00$	1.7988e-05	1.2675e-05	8.4025e-06	4.9436e-06	2.1660e-06
	0.19 s	0.19 s	0.20s	0.20s	0.21 s
$t = 0.80$	4.3640e-07	2.1467e-07	1.0012e-07	4.1661e-08	1.2896e-08
	0.17 s	0.18 s	0.17 s	0.18 s	0.18 s

4. Applications and results

In this section, numerical examples are presented with different kinetics. We utilized the fourth-order difference schemes proposed in Section 3 for the approximation of the Riesz derivatives. The improved exponential time-differencing Runge-Kutta method of order four as suggested in [24] is used to advance in time. All the computational experiments are carried out in Matlab R2019a on a PC equipped with an Intel Core i7 CPU, 4.0 GHz with 16.0 Gbyte of RAM under Windows 10 software.

4.1. Riesz-space model with Turing patterns

We first consider the integer-order reaction-diffusion system which was proposed by Barrio et al. [8], but modeled with the Riesz fractional operator as

$$\begin{aligned}
 \frac{\partial u}{\partial t} &= D_u \Delta^\beta u + au(1 - r_1 v^2) + v(1 - r_2 u), \\
 \frac{\partial v}{\partial t} &= D_v \Delta^\beta v + bv \left(1 + \frac{ar_1}{b} uv \right) + u(c + r_2),
 \end{aligned} \tag{4.73}$$

where D_u and D_v are the diffusion coefficients of u and v species at time t and position x , respectively. These coefficients indicate a conservation relation between the two chemical products [8], [51]. The key interaction parameters in (4.73) are r_1 and r_2 as each favors the formation of stripes and spots or dot-like patterns, respectively. Another key parameter which plays an important role in the simulation process is the fractional index β . Variation of this parameter can lead to various Turing's patterns. The parameters a, b and c are related to production and depletion of chemicals. The classical form of model (4.73) has been used mainly to study pattern formation in reaction-diffusion systems. In addition, it has been used to study transitions between fish patterns that go from stripes to spots, for example, the pseudoplatystoma fish species [51].

For numerical results to mimic some of these physical behaviors, we fix the parameters at $D_u = 2.322e - 03$, $D_v = 0.0045$, $a = 0.899$, $b = -0.91$, $c = -0.899$, $r_1 = 3.5$ and $r_2 \in [0, 2]$. In the experiment, parameter β is allowed to be varied. For all the experiments in one and two dimensions, we utilized the Matlab random initial conditions. The one-dimensional results with variation of r_2 is given in Fig. 3, with evidence of spatiotemporal and chaotic oscillations as r_2 increases. Evidence of Turing patterns are shown in Fig. 4, Fig. 5, Fig. 6. It was observed that when $r_2 \rightarrow 0$, the simulation experiments gives stripes or spiral-like structures, but the dynamics transform from stripes or spirals as $r_2 \gg 0$. Finally, in Fig. 6, as $\beta \rightarrow 1$, we obtained a more bold and pronounced patterns.

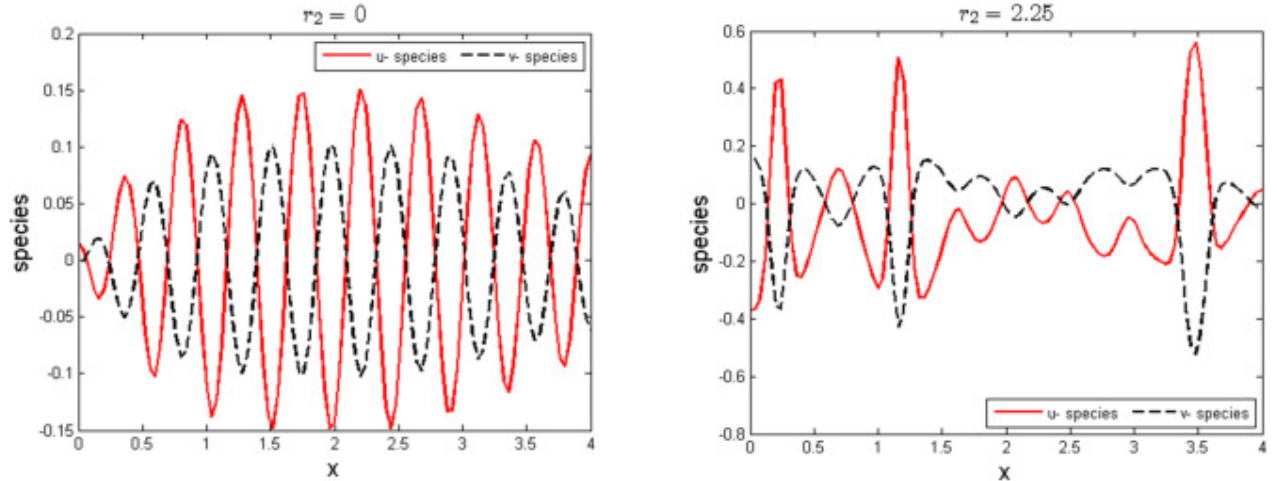


Fig. 3. One-dimensional results of (4.73) showing the evolution of species in space. With fixed $\beta = 1.55$ and $r_2 = 0, 2.25$ we obtain both spatiotemporal and chaotic behaviors of species, respectively.

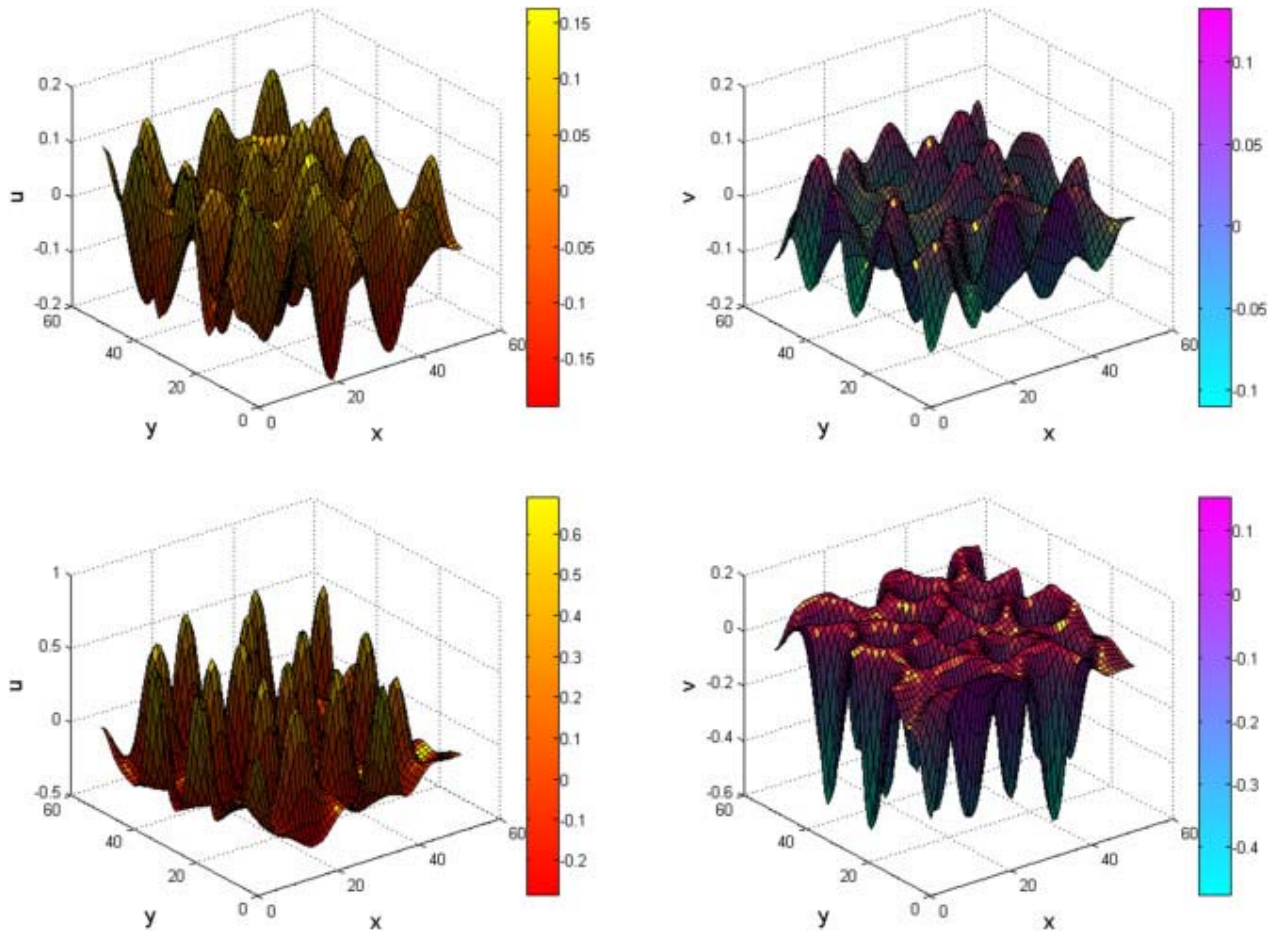


Fig. 4. Two-dimensional surface plots for model (4.73). The upper and lower rows correspond to $r_2 = 0$ and $r_2 = 1.57$, respectively. The fractional parameter is fixed at $\beta = 1.63$. Simulation runs for $N = 100$ and final time $t = 50$.

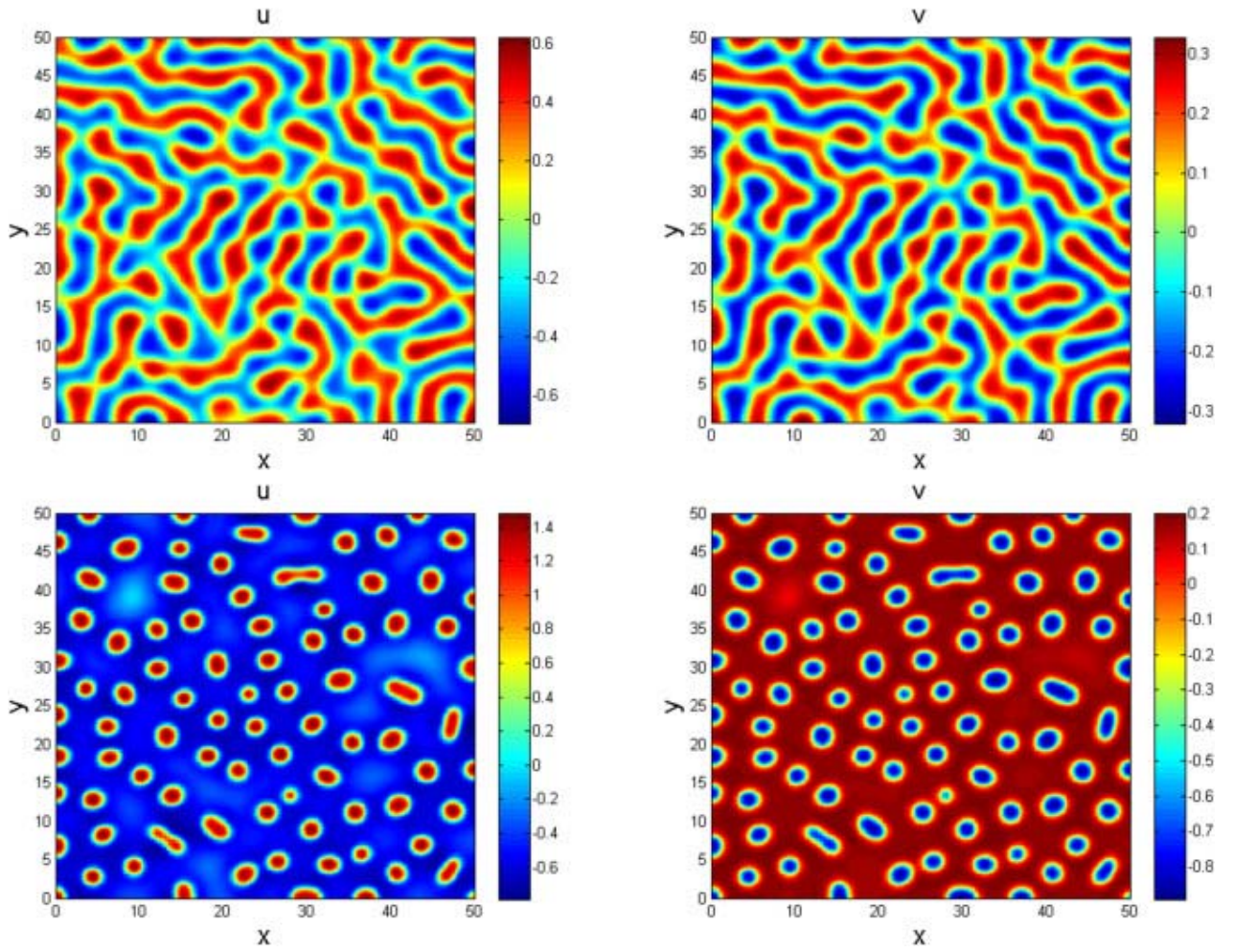


Fig. 5. Two-dimensional snapshots for model (4.73). The upper and lower rows correspond to $r_2 = 0.005$ and $r_2 = 2.50$, respectively. The formation of Turing stripes and spots patterns are noticeable.

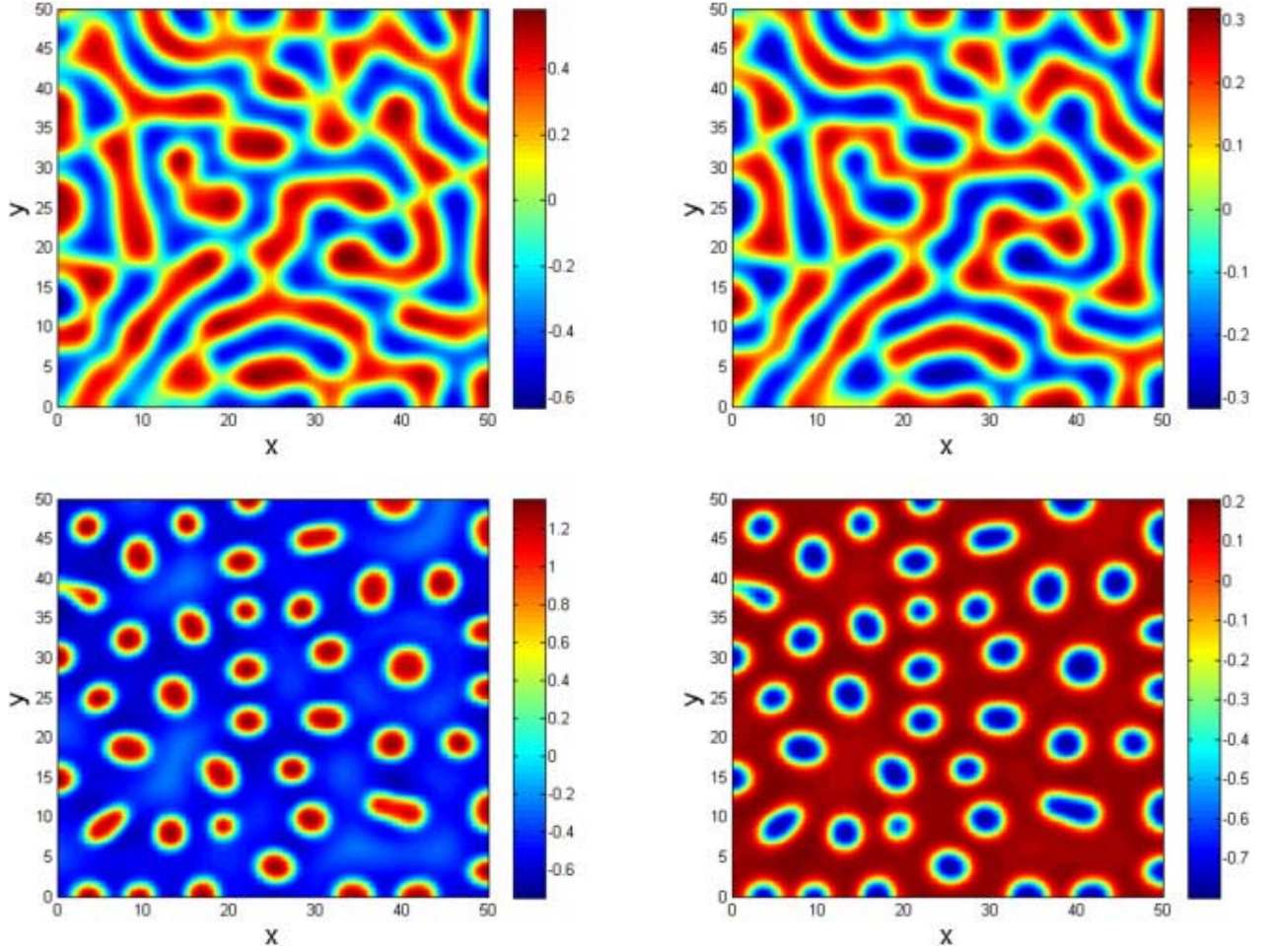


Fig. 6. Snapshots for model (4.73) in 2D with $\beta = 1.87$. Turing stripes and spots patterns are evident(4.75)

4.2. Riesz-space model with labyrinthine patterns

One of the most interesting and noticeable group of patterns that arise naturally in system of catalytic reactions are growing labyrinthine patterns [20], [36], [45]. Labyrinthine patterns provide a beautiful pattern formation scenarios at the neighborhood of the equilibrium state. Structures of this form have been studied in different gradient systems such as ferrofluids, turbulence, garnet layers, and block copolymers, see [20] and references therein. Beginning from a non-axisymmetric initial condition strongly curved portions spread more faster and the pattern lengthens. Regions of high concentrations repel, so from the periodicity of the domain, the patterns turn inward until an equilibrium is achieved.

The Riesz-space fractional reaction-diffusion equations for this example take the form

$$\begin{aligned}
\frac{\partial u}{\partial t} &= \Delta^\beta u + u - u^3 - v, \\
\frac{\partial v}{\partial t} &= D\Delta^\beta v + \epsilon(u - \alpha_1 v - \alpha_0),
\end{aligned} \tag{4.74}$$

where u and v are the scalar real fields which denote the activator and inhibitor, respectively. Parameter $\epsilon > 0$ is the ratio between the time scales associated with the two fields. Models of this type have extensively been studied in the context of excitable media where $0 < \epsilon < 1$, $D \geq 0$ is the ratio between the two diffusion coefficients, that is, $D = D_u/D_v$. When $D \gg 1$, a stable labyrinthine patterns is known to arise from the FitzHugh-Nagumo type reaction diffusion equations. For the parameters $\alpha_1 > 0$ and α_0 , we choose α_0 and α_1 in such a way that the model has two stable uniform steady states, namely, the points $E^- = (u^-, v^-)$ and $E^+ = (u^+, v^+)$ which correspond to a down and an up states, respectively. The variation of parameters α_0 , α_1 , $\beta \in (1, 2)$, D lead one from one regime to another. In the experiment, we utilize the homogeneous boundary conditions pinned at the extremes of domain size $x, y \in [-L, L]$ with $L = 100$, and the

following initial conditions. Here, $v^- = \frac{u^- - \alpha_0}{\alpha_1}$ is obtained from, u^- which is the smallest real root of the cubic $\alpha_1 u^3 + u(1 - \alpha_1) - \alpha_0 = 0$. It is obvious that the solution of $u(x, y, t)$ and $v(x, y, t)$ of (4.74) depend on the five parameters α_0 , α_1 , ϵ , D and β , but we will avoid displaying this dependence unless we specifically wish to address it. Also, it should be mentioned that other patterns apart from those ones displayed in Fig. 7, Fig. 8 are obtainable, depending on the choice of other parameters. Here, only fractional parameter β is varied with time. In Fig. 7, we display the distribution of the two chemical species for some values of β as reported in the Caption for time $t = 5000$. Other parameters are fixed as $\Delta t = 0.1$, $N = 128$, $\alpha_0 = -0.1$, $\alpha_1 = 2$, $\epsilon = 0.05$, and $D = 4$. Having observed that the distribution of u and v are almost similar as shown in Fig. 7, we continue our analysis by reporting only the distribution of u - species. In Fig. 8, we obtained the numerical results in rows 1-4 with $\beta = [1.58, 1.76, 1.88, 1.98]$. The distributions in column 1 are obtained with $t = 100, 200$, column 2 with $t = (300, 400, 600, 800)$, while the last column depicts the result with final simulation time $t = 10,000$ [53].

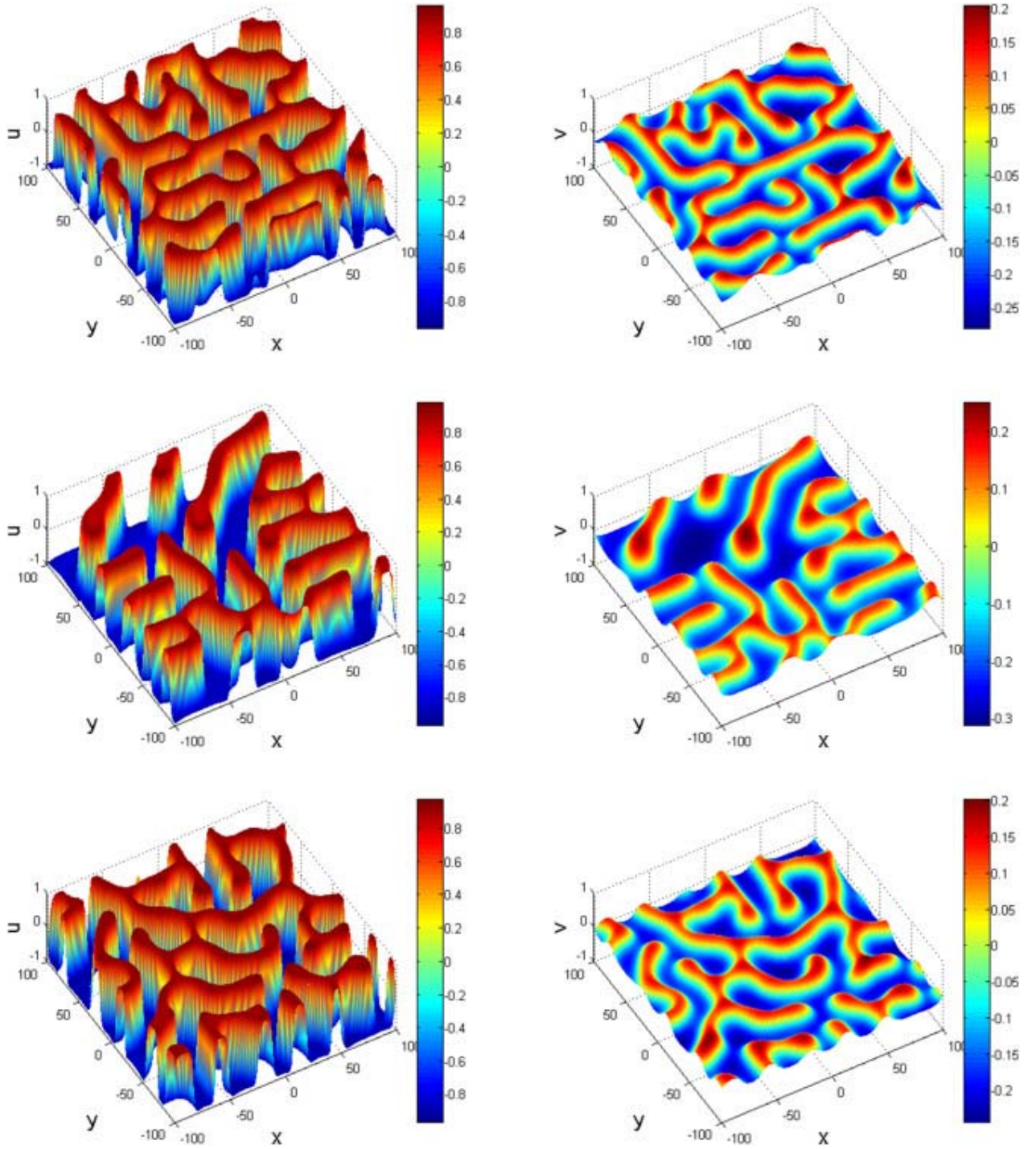


Fig. 7. Surface distribution of system (4.74) in 2D with different instances of β . The upper-, middle-, and lower-rows correspond to $\beta = 1.98, 1.76, 1.94$, respectively.

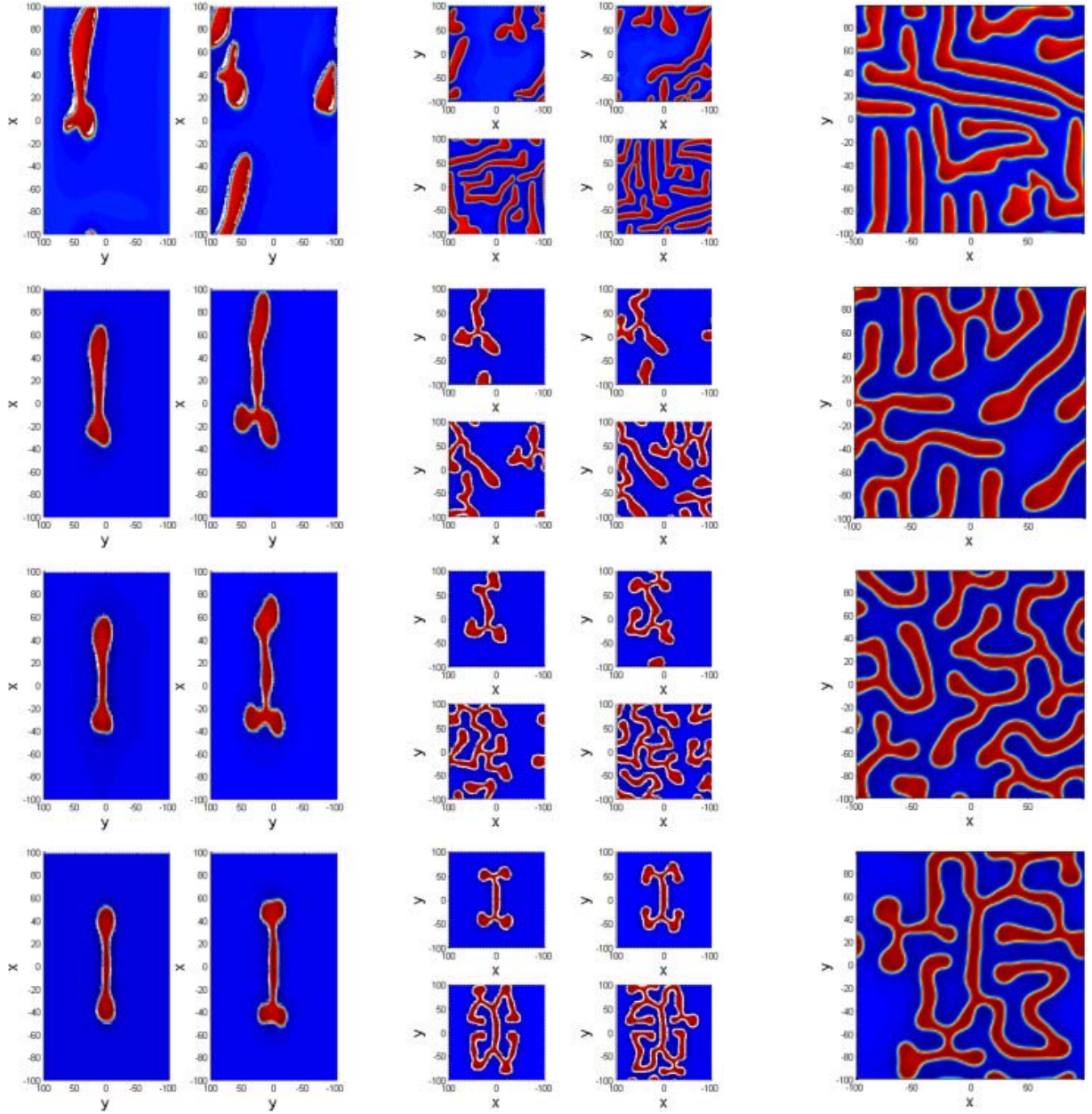


Fig. 8. Two-dimensional distribution of u -species for the Riesz fractional activator-inhibitor model (4.74) for different values of β and final simulation time.

Applicability and accuracy of the suggested scheme is further investigated when applied to a system of eqs. (4.74) by reporting the maximum error computed at some specific points in the experiment. To check the convergence we fix the parameters and simulate the experiment with a gold-standard run computed with $\Delta t = 10^{-5}$, with increasing time (t) and step-size (h) and $\beta = 1.90$ to obtain the following results.

```

Now at t=0.1, using h = 0.1 (errmax=7.4475e-12)
Now at t=0.6, using h = 0.5 (errmax=1.7641e-08)
Now at t=1.5, using h = 0.9 (errmax=4.0298e-07)
Now at t=2.4, using h = 0.9 (errmax=7.9356e-07)
h = 0.9 WAS REJECTED (errmax=0.0045901)
Now at t=2.7285, using h = 0.32848
(errmax=1.1725e-08)
h = 0.9 WAS REJECTED (errmax=0.002818)
Now at t=3.0996, using h = 0.37109
(errmax=2.7178e-08)
h = 0.9 WAS REJECTED (errmax=0.0010966)
Now at t=3.5694, using h = 0.46985
(errmax=1.1614e-07)
h = 0.9 WAS REJECTED (errmax=0.0046936)
Now at t=3.8961, using h = 0.32666
(errmax=3.0241e-08)
h = 0.9 WAS REJECTED (errmax=0.002918)
Now at t=4.2639, using h = 0.36787
(errmax=7.2094e-08)

```

(3.42)

```

Now at t=0.1, using h = 0.1 (errmax=2.4447e-10)
Now at t=0.6, using h = 0.5 (errmax=4.6348e-07)
Now at t=1.5, using h = 0.9 (errmax=1.1053e-06)
Now at t=2.4, using h = 0.9 (errmax=3.1929e-06)
h = 0.9 WAS REJECTED (errmax=1.2154)
Now at t=2.8691, using h = 0.46906
(errmax=1.0549e-07)
Now at t=3.2312, using h = 0.36213
(errmax=1.7193e-06)
h = 0.72107 WAS REJECTED (errmax=0.0052674)
Now at t=3.672, using h = 0.44079
(errmax=7.1844e-08)
h = 0.9 WAS REJECTED (errmax=0.15707)
Now at t=3.7168, using h = 0.13581
(errmax=1.8654e-08)
h = 0.67906 WAS REJECTED (errmax=0.0007125)
Now at t=4.1117, using h = 0.39486
(errmax=8.8583e-07)
h = 0.9 WAS REJECTED (errmax=0.021736)
Now at t=4.3344, using h = 0.22268
(errmax=2.179e-08)
h = 0.9 WAS REJECTED (errmax=0.012762)
Now at t=4.5888, using h = 0.25438
(errmax=4.9695e-08)

```

(3.68)

5. Conclusion

In this work, two higher-order numerical techniques for the approximation of the Riesz fractional-order operator have been considered. The formulation, analysis, and convergence of these methods are well examined. We choose to illustrate the numerical algorithms using a couple of non-trivial examples from the literature on reaction-diffusion equations. Hence, the method is tested on two important Riesz space fractional reaction-diffusion models. In the first example, we observe the Turing stripes and spots patterns arising from the BVAM model, it was also observed that pattern generation in classical order models are similar to the fractional-order cases. In the second example, we consider the Labyrinthine patterns evolved from the special case of the FitzHugh-Nagumo type of reaction-diffusion system. It is worth mentioning that other behavioral patterns are obtainable for these equations in other parameter regimes than those used in this paper.

CRedit authorship contribution statement

The idea was conceived by KM. Owolabi, KM. Saad and E. Pindza. Initial draft was written by KMO, initial analysis was carried out by M. Alqhatani, Computation of results was done by E. Pindza. All authors proofread and approve the final version.

Declaration of competing interest

We declare that our paper is solely prepared for the Special issue “Mathematical Modelling and Simulation of Biological Systems (MMSimBio)” and to be submitted to Chaos Solitons and Fractals only.

Acknowledgment

The authors are thankful to the Deanship of Scientific Research at Najran University for funding this work under the General Research Funding program grant code (NU/RG/SERC/11/3).

Data availability

No data was used for the research described in the article.

References

1. Abidemi A, Owolabi KM, Pindza E. Modelling the transmission dynamics of Lassa fever with nonlinear incidence rate and vertical transmission. *Physica A*. 2022; 597:127259.
2. Alqhtani M, Owolabi KM, Saad KM. Spatiotemporal (target) patterns in sub-diffusive predator-prey system with the caputo operator. *Chaos, Solitons Fractals*. 2022; 160:112267.
3. Arqub OA, et al. Development of the reproducing kernel hilbert space algorithm for numerical pointwise solution of the time-fractional nonlocal reaction-diffusion equation. *Alex Eng J*. 2020; 61:10539–50.
4. Arqub OA, et al. A numerical algorithm for the solutions of ABC singular Lane-Emden type models arising in astrophysics using reproducing kernel discretization method. *Mathematics*. 2020;8(6):923.
5. Atangana A. *Derivative with a new parameter: theory*. Methods and Applications: Academic Press, New York; 2016.
6. Atangana A. *Fractional operators with constant and variable order with application to geo-hydrology*. New York: Academic Press; 2017.
7. Atangana A, Owolabi KM. New numerical approach for fractal differential equations. *Math Model Nat Phenom*. 2018; 13:3.
8. Barrio RA, Varea C, Aragon JL, Maini PK. A two-dimensional numerical study of spatial pattern formation in interacting Turing systems. *Bull Math Biol*. 1999;61: 483–505.
9. Bayin SS. Consistency problem of the solutions of the space fractional Schrödinger equation. *J Math Phys*. 2013; 54:092101.
10. Benson DA, Wheatcraft SW, Meerschaert MM. The fractional-order governing equation of Lévy motion. *Water Resour Res*. 2000;36(6):1413–23.

11. Bueno-Orovio A, Kay D, Burrage K. Fourier spectral methods for fractional-in-space reaction-diffusion equations. *BIT Numer Math.* 2014; 54:937–54.
12. Cai M, Li C. On riesz derivative. *Fract Calc Appl Anal.* 2019; 22:287–301.
13. Celik C, Duman M. Crank-nicolson method for the fractional diffusion equation with the Riesz fractional derivative. *J Comput Phys.* 2012; 231:1743–50.
14. Das S. A note on fractional diffusion equations. *Chaos Solitons Fractals.* 2009;42(4): 2074–9.
15. Dhawan S, et al. A chebyshev wavelet collocation method for some types of differential problems. *Symmetry.* 2021;13(4):156.
16. Ding H, Li C, Chen Y. High-order algorithms for Riesz derivative and their applications (I). *Abstract and Applied Analysis.* 2014; 2014:653797 1-18.
17. Ferdi Y. Some applications of fractional order calculus to design digital filters for biomedical signal processing. *J Mech Med Biol.* 2012;12(02):1240008.
18. Gorenflo R, Mainardi F, Scalas E, Raberto M. Fractional calculus and continuous-time finance. III. The diffusion limit. *Math Finance (Konstanz, 2000).* 2001:171–80.
19. Guo BL, Pu XK, Huang FH. Fractional partial differential equations and their numerical solutions. Beijing, China: Science Press; 2011.
20. Hagberg A, Meron E. From labyrinthine patterns to spiral turbulence. *Phys Rev Lett.* 1994;72:2494–7.
21. Herrmann R. Fractional calculus: an introduction for physicists. Singapore: World Scientific; 2011.
22. Huang F, Guo B. General solutions to a class of time fractional partial differential equations. *Appl Math Mech.* 2010; 31:815–26.
23. Inan B, et al. Analytical and numerical solutions of mathematical biology models: the Newell-Whitehead-Segel and Allen-Cahn equations. *Math Methods Appl Sci.* 2020; 43:2588–600.
24. Kassam AK, Trefethen LN. Fourth-order time stepping for stiff PDEs. *SIAM J Sci Comput.* 2005; 26:1214–33.
25. Kilbas AA, Srivastava HM, Trujillo JJ. Theory & applications of fractional differential equations. Amsterdam: Elsevier; 2006.
26. Kwásnicki M. The equivalent definitions for the fractional Laplacian operator. *Fract CalcAppl Anal.* 2017; 20:7–51.
27. Li C, Beaudin J. On the generalized Riesz derivative. *Mathematics.* 2020; 8:1089.
28. Li CP, Zeng FH. Numerical Methods for Fractional Calculus. Boca Raton, USA: CRC Press; 2015.
29. Liu F, Anh V, Turner I, Zhuang P. Time fractional advection-dispersion equation. *J Appl Math Comput.* 2003;13(1–2):233–46.
30. Liu F, Anh V, Turner I. Numerical solution of the space fractional Fokker-Planck equation. *J Comput Appl Math.* 2004;166(1):209–19.
31. Liu JG, Zhang YF. Analytical study of exact solutions of the nonlinear Korteweg-de Vries equation with space-time fractional derivatives. *Mod Phys Lett B.* 2018;32: 1850012.
32. Liu JG, Yang XJ, Feng YY, Zhang HY. Analysis of the time fractional non-linear diffusion equation from diffusion process. *J Appl Anal Comput.* 2020; 10(3): 1060C1072.
33. Mainardi F. Fractional calculus and waves in linear viscoelasticity: an introduction to mathematical models. London: World Scientific; 2010.
34. Mandelbrot B. The fractal geometry of nature. New York, NY, USA: Henry Holt and Company; 1982.

35. Meerschaert MM, Tadjeran C. Finite difference approximations for fractional advection-dispersion flow equations. *J Comput Appl Math.* 2004; 172:65–77.
36. Meron E, Bäär M, Hagberg A, Thiele U. dynamics in catalytic surface reactions. *Catalysis Today.* 2001; 70:331–40.
37. Metzler R, Klafter J. Boundary value problems for fractional diffusion equations. *Physica A.* 2000;278(1–2):107–25.
38. Metzler R, Klafter J. The random walk’s guide to anomalous diffusion: a fractional dynamics approach. *Phys Rep.* 2000;339(1):1–77.
39. Metzler R, Klafter J. The restaurant at the end of the random walk: Recent developments in the description of anomalous transport by fractional dynamics. *J Phys A Math Gen.* 2004; 37: R161.
40. Oldham KB, Spanier J. *The fractional calculus.* New York: Academic Press; 1974.
41. Ortigueira MD. Riesz potential operators and inverses via fractional centred derivatives. *Journal Abbreviation: Int J Math Math Sci.* 2006;2006(48391):1–12.
42. Ortigueira MD. Two-sided and regularised Riesz-Feller derivatives. *Math Methods Appl Sci.* 2021; 44:8057–69.
43. Owolabi KM. Mathematical analysis and numerical simulation of patterns in fractional and classical reaction-diffusion systems. *Chaos Solitons Fractals.* 2016;93: 89–98.
44. Owolabi KM, Atangana A. Numerical solution of fractional-in-space Schrödinger equation with the Riesz fractional derivative. *Eur Phys J Plus.* 2016; 131:335.
45. Owolabi KM. Robust and adaptive techniques for numerical simulation of nonlinear partial differential equations of fractional order. *Commun Nonlinear Sci Numer Simulat.* 2017; 44:304–17.
46. Owolabi KM, Atangana A. Higher-order solvers for space-fractional differential equations with Riesz derivative. *Discrete Contin Dyn Syst S.* 2019; 12:567–90.
47. Owolabi KM. Numerical simulation of fractional-order reaction-diffusion equations with the Riesz and Caputo derivatives. *Neural Comput Appl.* 2019; 34:4093–104.
48. Owolabi KM. High-dimensional spatial patterns in fractional reaction-diffusion system arising in biology. *Chaos Solitons Fractals.* 2020; 34:109723.
49. Owolabi KM, Pindza E, Atangana A. Analysis and pattern formation scenarios in the superdiffusive system of predation described with Caputo operator. *Chaos Solitons Fractals.* 2021; 152:111468.
50. Owolabi KM, Baleanu D. Emergent patterns in diffusive Turing-like systems with fractional-order operator. *Neural Comput Appl.* 2021; 33:12703–20.
51. Owolabi KM. Computational analysis of different *Pseudoplatystoma* species patterns the Caputo-Fabrizio derivative. *Chaos Solitons Fractals.* 2021; 144:110675.
52. Peaceman DW, Rachford HH. The numerical solution of parabolic and elliptic differential equations. *J Soc Ind Appl Math.* 1955; 3:28–41.
53. Pindza E, Owolabi KM. Fourier spectral method for higher order space fractional reaction-diffusion equations. *Commun Nonlinear Sci Numer Simul.* 2016; 40: 112–28.
54. Podlubny I. *Fractional differential equations.* New York: Academic Press; 1999.
55. Raberto M, Scalas E, Mainardi F. Waiting-times and returns in high-frequency financial data: an empirical study. *Physica A.* 2002; 314:749–55.
56. Rashid S, et al. An approximate analytical view of physical and biological models in the setting of Caputo operator via Elzaki transform decomposition method. *J Comput Appl Math.* 2022; 413:114378.
57. Saichev AI, Zaslavsky GM. Fractional kinetic equations: solutions and applications. *Chaos.* 1997; 7:753–64.

58. Samko SG, Kilbas AA, Marichev OI. Fractional integrals and derivatives: theory and applications. Amsterdam: Gordon and Breach; 1993.
59. Scalas E, Gorenflo R, Mainardi F. Fractional calculus and continuous-time finance. *Physica A*. 2000;284(1–4):376–84.
60. Tadjeran C, Meerschaert MM. A second-order accurate numerical method for the two-dimensional fractional diffusion equation. *J Comput Phys*. 2007; 220:813–23.
61. Tian WY, Zhou H, Deng WH. “A class of second order difference approximation for solving space fractional diffusion equations. *Math Comput*. 2015; 84:1703–27.
62. Wyss W. The fractional Black-Scholes equation. *Fract CalculusAppl Anal*. 2000;3: 51–61.
63. Yang Q, Liu F, Turner I. Numerical methods for fractional partial differential equations with Riesz space fractional derivatives. *App Math Model*. 2010; 34:200–18.
64. Yuste SB, Acedo L, Lindenberg K. Reaction front in an reaction-subdiffusion process. *Phys Rev E*. 2004;69(3):036126.
65. Zaslavsky GM. Chaos, fractional kinetics, and anomalous transport. *Phys Rep*. 2002; 371(6):461–580.
66. Zhang W. Finite difference methods for partial differential equations in science computation. Beijing, China: Higher Education Press; 2006.
67. Zhang H, Liu F. The fundamental solutions of the space, space-time Riesz fractional partial differential equations with periodic conditions. *Numer Math*. 2007;16: 181–92.
68. Zhang H, Liu F, Anh V. Galerkin finite element approximation of symmetric space-fractional partial differential equations. *Appl Math Comput*. 2010; 217:2534–45.